# AutomatedDetection of Wet Aged Related Macular Degeneration Using Optical Coherence Tomographic Images

by
AnamHaq
2011-NUST-MS PhD- ComE-04
MS-69


Submitted to the Department of Computer Engineering in fulfillment of the requirements for the degree of

MASTER OF SCIENCE
in
COMPUTER ENGINEERING

Thesis Supervisor
Prof. Dr. Shoab Ahmad Khan

Department of Computer Engineering
College of Electrical & Mechanical Engineering
National University of Sciences& Technology
Islamabad
May, 2014

# AutomatedDetection of Wet Aged Related Macular Degeneration Using Optical Coherence Tomographic Images

by
AnamHaq
2011-NUST-MS PhD- ComE-04
MS-69

Submitted to the Department of Computer Engineering in fulfillment of the requirements for the degree of

MASTER OF SCIENCE
in
COMPUTER ENGINEERING

Thesis Supervisor:
Prof. Dr. Shoab Ahmad Khan

Thesis Supervisor's Signature:_____

Department of Computer Engineering
College of Electrical & Mechanical Engineering
National University of Sciences& Technology
Islamabad
May, 2014

# CHAPTER 1 INTRODUCTION

## 1.1 Overview

With the rapid development in the field of medicine new technologies are invented in order to examine the body. These machines use medical imaging to diagnose or detect diseases. Most common used medical imaging technologies are Optical Coherence Tomographic images (OCT), Fundus Fluorescein Angiography (FFA), Computed Tomography, Magnetic Resonance Imaging, Mammography, diagnostic ultrasound, and X-ray, etc. (shown in fig 1.1). Each one of them gives certain information about the human body which helps in further diagnosis of a particular disease. For instance:

1. X-ray,MRI and ultrasound yield information that helps the radiologist to analyze and evaluate results in short time.
2. Mammography is used to detect breast cancer and lung cancer etc.

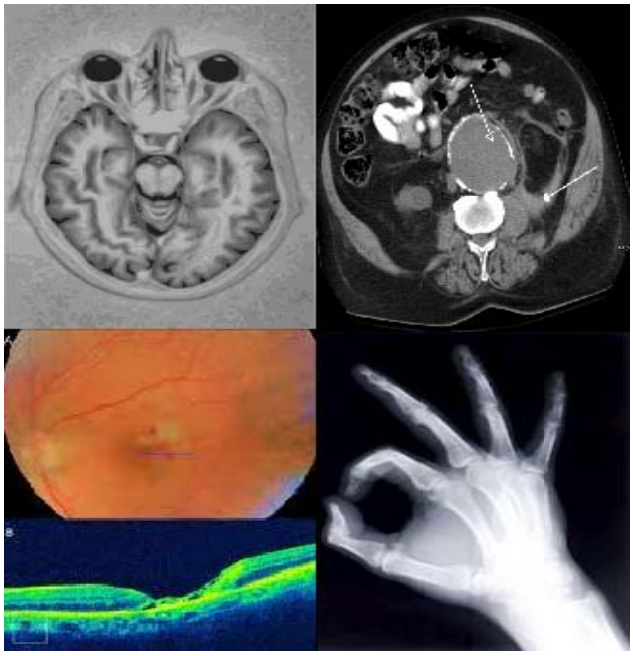

**Figure 1.1 Medical Imaging Technologies [1]**

Medical imaging has undergone major development in the past years. Computer aided diagnostic systems are used all over the world for research and clinical purposes. These systems operate on digital medical images and the basic aim behind these systems is to facilitate doctors and patients.

At present computer aided systems cannot substitute doctors rather they provide a supporting role. The presence of doctor to interpret medical images is necessary. However, some surgeries are done by using computer aided robots (shown in figure 1.2).

**Figure 1.2 Computer Aided Robots [1]**

Wet Aged related macular degeneration is a type of macular disorder. It is caused by the detachment of retinal pigment epithelium and CNV. The person suffering from it has a high risk of losing his/her central vision. The difference in the central vision of patients having healthy eye and diseased eye is shown in figure 1.3. Wet aged related macular degeneration can be diagnosed by using FFA and OCT medical imaging techniques. The most recent approach used by the doctors to detect this disease is by using OCT machine.

**Figure 1.3 (a)Healthy Eye Vision, (b) Dry AMD eye vision, and (c) Wet AMD eye vision [12]**

Very few research works has been previously done in detecting wet aged related macular degeneration using optical coherence tomographic images. Most work on OCT images is done on the removal of speckle noise and automated segmentation of retinal layers. Our system not uses the basic Computer Aided system approach and detects the abnormalities from the medical images that are used to classify the diseased eye from the healthy eye.

## 1.2 Motivation

Wet aged related macular degeneration is the third most leading cause of blindness after cataract and glaucoma. But in industrialized countries, it is the most leading cause of blindness for people who are aged 65 years above. The statistical ratio of blindness prevalence in Pakistan is from 2.1% to 8.7%. This ratio can be large due to the lack of resources and information in rural areas of Pakistan.

Doctor to patient ratio in Pakistan is 1:1000 which proves that the facility of health care is very low. Aside from that there are very rare technical people present to handle medical imaging instruments. Seeing such facts, research work in this field will prove to be very useful.

Optical coherence tomographic machines are very expensive and are very rarely found in Pakistan. Only some Hospitals out of hundreds have them. The automated design systems will not only store patient's medical images, but also perform a self-diagnosis, thus providing remote

health care facility in rural areas of Pakistan. By putting a small effort in designing such systems will not only provide telemedicine facilities but they can also facilitate us in improving health care in rural parts of our country.

Development of such systems at local level is attracting the eyes of researchers, medical professionals and students. Designing of such computer aided medical systems will also enable the engineer and doctor's collaboration which will bridge the gap between the research engineers, medical specialists and industries.

The major aim of this algorithm is to provide the self-diagnostic and real time screening for patients suffering from wet aged related macular degeneration.

## 1.3 Scope and Objective

The research in medical imaging is of great importance, as it not only facilitate the ophthalmologist, but will also bridge the gap between the engineer researchers and the industries. Some of the major objectives regarding this research work are mentioned below:

1. Designing of an automated system that will detect wet aged related macular degeneration by using image processing and pattern recognition techniques.
2. The objective is to facilitate physicians in time consuming screening of OCT images not to bypass the physician's role.
3. Designing algorithm that provides ease of access, cost effective and non-invasive treatment of patients.
4. To aware students and researchers regarding the possibility of work that can be achieved in this field.
5. To provide researchers with the medical (Ophthalmology) knowledge.
6. Encourage industry to support such projects that will encourage health care in Pakistan.

## 1.4 Challenges

The major challenged with designing of this system was that there is very less amount of research work available regarding detection of wet aged related macular degeneration by using

optical coherence tomography images. The researchers are focusing more on the segmentation of retinal layers and removal of speckle noise in OCT images as it is also a major concern. But using keen observation, we were able to develop a system that detects abnormalities from the OCT images that are linked to wet age related macular degeneration.

The second most challenging situation was that there is no publicly available set of OCT images. This situation was overcome with the help of the Armed Forces institute of ophthalmology Rawalpindi, Pakistan. They provide us with the required medical images.

## 1.5 Organization of Thesis

The thesis structure is as follows:

Chapter 2 provides the readers with the basic introduction of eye structure. It then describes the functions and components of the macula, followed by macular disorder and how valuation of this disorder is done. The chapter further describes various types of macular disorder mainly focusing on Wet aged related macular degeneration. It also gives a detailed description of Optical coherence tomographic imaging.

Chapter 3 provides a literature review regarding previous work done in the detection wet end and on optical coherence tomographic images. Chapter 4 gives the detail structure of the designed system. It explains the proposed techniques and algorithm development. It gives the description of removing speckle noise; extraction region of interest, segmenting abnormalities related to wet age related macular degeneration using morphological operations, extracting defined feature set and classification of healthy and diseased eye.

Chapter 5 elaborates the results and graphs achieved using the proposed system and also provide the comparison with the previously designed system.Chapter 6 contains the concluding remarks and future work to be done.

## 1.6 Summary

Medical imaging advancement and computer science enables us to enhance the ability of machines for detecting or diagnosing various diseases. The work achieved by me enables us to

correctly detect the presence or absence of wet age related macular degeneration. The system is tested and performance is evaluated using statistical feature measures. Methodology used is exclusive and can be used on detecting other macular diseases by only using different feature set.

# CHAPTER 2 MACULAR DISORDER

## 2.1 Anatomy of Eye

The eye is connected and dependent on the brain to interpret what we saw. Light reflected from the object we are seeing passes through the front of the eye, which is called cornea to the eye lens. Cornea and lens further help the light to focus onto the back of the eye known as the retina. The cells present in the center of the retina absorb the light and convert it into electrochemical impulses. These impulses reached the brain through the optic nerve [1]. The main components of eye are shown in figure 2.1 and are explained below.

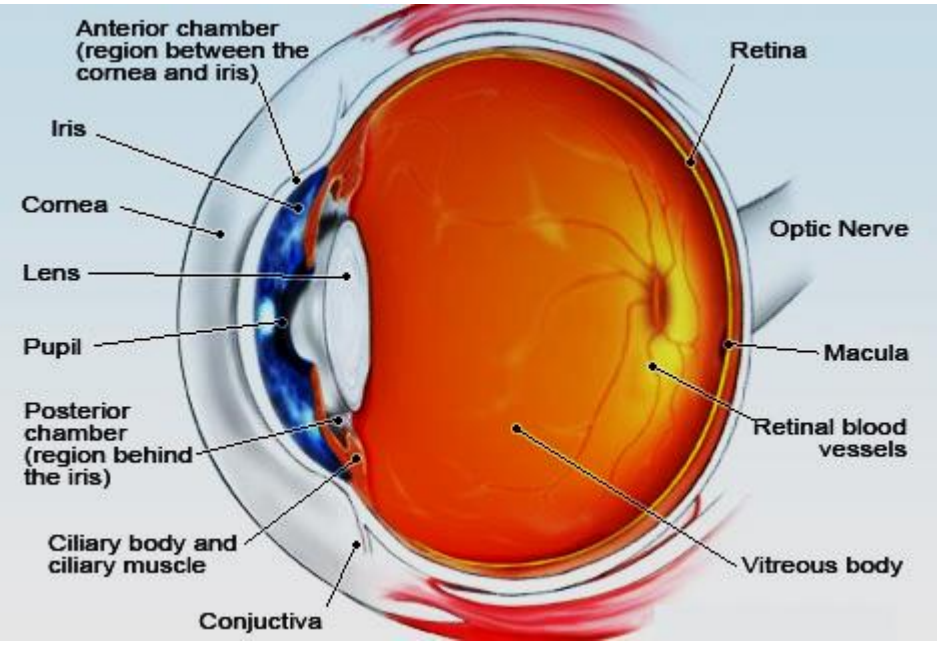


**Figure 2.1 Anatomy of Eye [2]**

1. **Cornea:** Eye Segment that is used to focus and transmit the light inside the eye.
2. **Iris:** The quantity of light required to enter in the eye is controlled by this eye colored portion.

3. **Pupil:** The light enters the eye through this black circular opening [2].
4. **Lens:** Light rays entering through the pupil are focused on the retina using lens (which is transparent) [2].
5. **Retina:** Retina is located on the back side of the eye. The function of the retina is to sense light and to create impulses. These impulses will then travel to the brain using optic nerve [2].
6. **Optic nerve**:This nerve plays the part of connecting the eye to the brain. It is also used as a medium to transmit electrical impulses. These impulses are created by the eye retina it provides the connection of the eye to the brain and connects the eye to the visual cortex of the brain [2].
7. **Vitreous**: This part of eye is like a gel. The eye's middle portion is occupied by this gel [2].
8. **Macula:** This part is located at the center of the retina. It contains sensitive cells of light, using which we are able to clearly view details [2].

### 2.1.1 Macula

It's essential to have a healthy macula in order to have normal central vision. Macula is built of light sensitive cells that are closely packed with each other, these cells are called rods and con. Out of these two, cells that are known as cons are the ones which are responsible for eye's vision. These cells are nurtured by the blood vessels layer called the choroid [3][4].

The tissue present at the outermost part of the retina is a layer known as retinal pigment epithelium (RPE). It contains only layer of cells which are hexagonal in cross-section. These cells have an outer non-pigmented and an inner pigmented apical section. Outer non pigmented basal element contains the nucleus and the inner pigmented apical section containing abundant melanosomes. The base of the RPE cells is in contact with the Bruch membrane [5].

RPE acts as an important passageway. The nutrients needed by the retina travel from the choroid to through RPE. Also the unwanted products are removed out of the retina, from choroid through RPE [4]. The cross sectional view of the retina is shown in figure 2.2.

The separation of RPE and The choriocapillaries is provided by the bruch membrane. Bruch Membrane is used by the RPE as a passage to discard the metabolic waste products out of the retina [5].

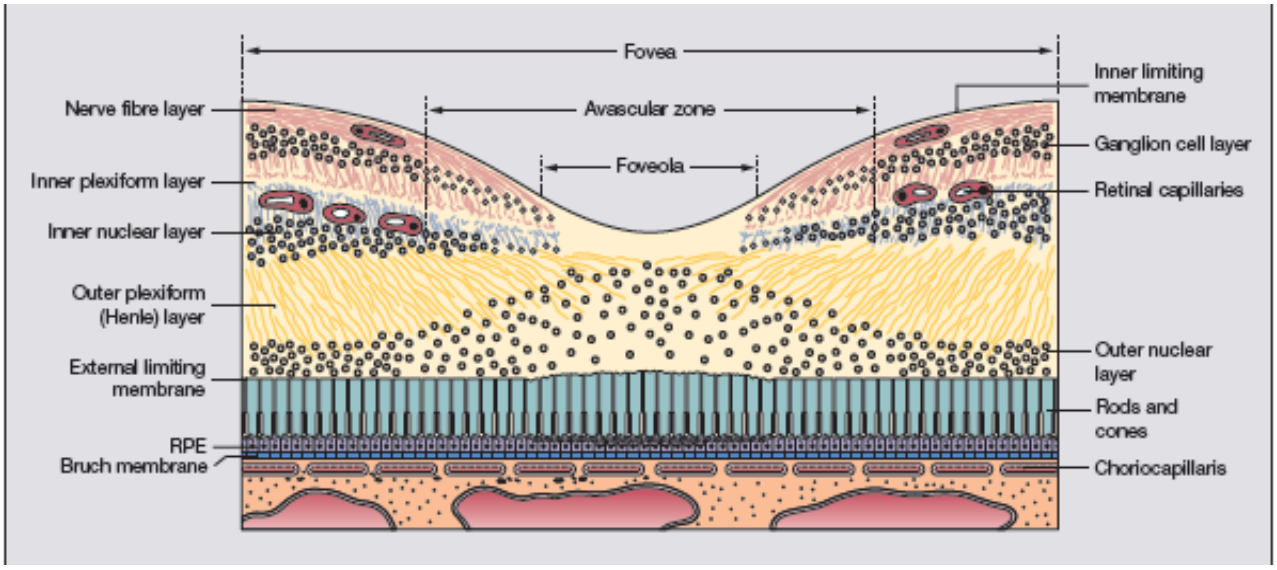


**Figure 2.2 Cross-section view of retina [2]**

### 2.1.1.1 Location, Shape and Components of Macula

**The macula** (Fig. 2.3 A) is a circular area located at the posterior pole, present in temporal vascular arcades. It ranges between 5 and 6 mm in diameters and sub serves the central 15–20° of the visual field [6].

**The fovea** (Fig. 2.3 B and Fig. 2.2)having a diameter of 1.5mm (about the same as the optic disk) can be seen in the middle of the macula as a depression on the retinal surface [6].

**The foveola** forms the fovea's central floor, which is 0.35mm in diameter. (Fig. 2.3C) [6].

In the centre of foveola's depression **umbo** is present. Umbo related to foveolar light reflex, and losing it will show an early damage sign [6].

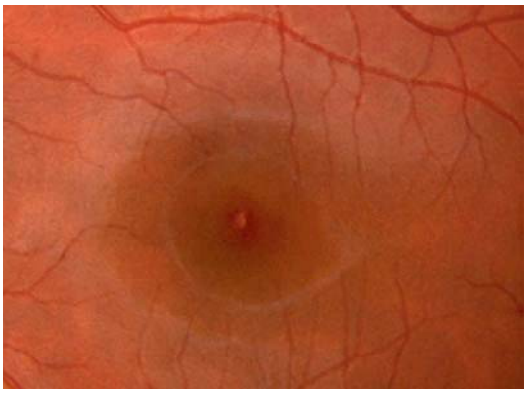

**Figure 2.3(A) Normal foveal light reflex [4]**

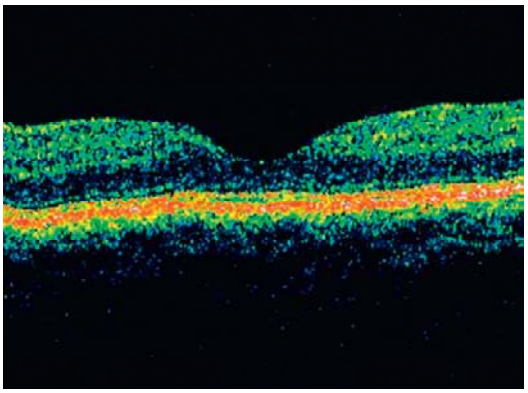

**Figure 2.3(B) OCT shows the foveal depression [4]**

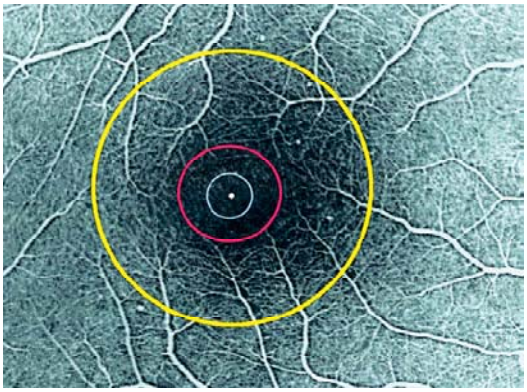

**Fig 2.3(C) Fovea (yellow circle); foveal avascular zone-approximate (red circle); foveola (lilac circle); umbo (central white spot) [4]**

## 2.2 Macular Disorder

As discussed above, it's the part of the eye that is responsible for a clear vision. Macular diseases are associated with the damaging of central vision. Impairment of the macula can bring serious consequences to a person. Some of the symptoms of macula disorder are given below [7][8]:

1. **Blurry Vision:** The person vision gets blurry and difficult to perform close work. These are the early symptoms of macular disorder. The macular disorder increases rapidly in conditions like CNV.
2. **Positive Scotoma:** In this symptom, patient's complaint about something which is blocking their central vision.

3. **Negative Scotoma:** It is similar to optic neuropathy. This symptom typically creates a missing area in the visual field.
4. **Metamorphopsia:** This symptom causes distortion of perceived images.
5. **Micropsia:** In this symptom the patient's complaint about the decreasing of image size. This is caused when foveal cones spread apart and is not much common.
6. **Macropsia:** In this symptom the patient's complaint about the increasing of image size. This is caused when the foveal cones are crowded together.
7. **Color:** This symptom disturbs the color discrimination of the patient.
8. **Difficulties related to dark adaptation:** In this symptom the patients suffer from poor vision in dim light.

## 2.3 Macular Functions Assessments

In order to test macular functionality two basic tests are performed first. These tests are

1. Visual Acuity and
2. Amsler Grid.

### 2.3.1 Visual Acuity

Visual acuity is defined as the clearness of vision. It is dependent on the sensitivity of the interpretative brain faculty and sharpness of the retinal focus inside the eye. Normally, visual acuity is 20/20 vision and the equivalent of it in metric is 6/6. At a distance of 6 meters the human eye that is able to separate lines 1.75 mm apart have normal performance, while 20/40 vision is considered as a good normal performance. Vision having 20/10 is twice as good as normal performance. [9] (Wikipedia)

Visual acuity is normally tested using a snellen chart which is shown in the figure 2.4 below.

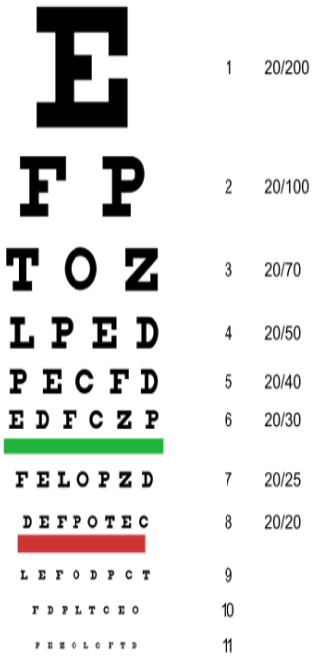


**Figure 2.4 Snellen Chart [9]**

### 2.3.2 Amsler Grid

There are various types of amsler grid. The most common form out of it is the one which is 10cm by 10cm grid and is printed on a white paper. This grid has a small black dot present at its center and are divided evenly into 0.5 cm by 0.5 squares as shown in figure 2.5 [11]. The steps to use amsler grid area:

- Step 1: Tell the patient to cover one of the eyes and to hold the amsler grid 30 cm away from him/her. The grid must be placed on the resting surface so the person can draw on it.
- Step 2: Ask this question: What is present at the center of the grid? If the patient is unable to see the dot present in the paper he/she is suffering from central scotoma.
- Step 3: If the person can see the central dot, the next question to be asked is: “Focus on the central dot and tell me if you can see from the corner of your eye all the four corners of the big box.

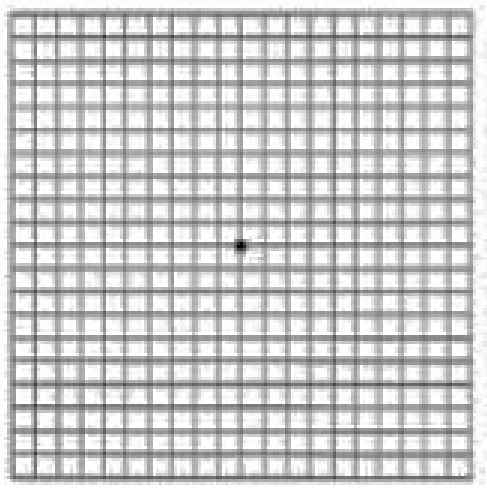

**Figure 2.5 Amsler Grid [10]**

- Step 4: continue your focus on the central dot: Can you find any small boxes which are missing? If you can? Please shade out the missing area.
- Step 5: Focus on the central dot: Do you see any distorted lines? If you can kindly draw over those lines.

Any kind of abnormalities in the above answer suggests the problem in the macula. Anyone can perform this test at home [10].

## 2.4 Types of Macular Disorder

The macula can be affected by a wide range of problems. The diseases which are caused due to macula disorder are:

1. Aged Related Macular Degeneration.
2. Age-related Macular Hole.
3. Polypoidal Choroidal Vasculopathy.
4. Central Serous Retinopathy.
5. Cystoid Macular Oedema.
6. Macular Epiretinal Membrane.
7. Degenerative Myopia.
8. Angioid Streaks.

9. Choroidal Folds.
10. Hypotony Maculopathy.
11. Vitreomacular Traction Syndrome.
12. Solar Maculopathy.
13. Idiopathic Choroidal Neovascularization.

### 2.4.1 Aged Related Macular Degeneration

Age-related macular degeneration (AMD) also referred to as age-related maculopathy (ARM), is a progressive disorder which affects the macula. This disease is marked by the presence of special type of clinical findings known as drowsiness, retinal pigment epithelium and choroidal neovascularization. The changes in these features show the presence of ARMD and later stage of this disease can cause vision impairment. AMD early detection is based on the presence of two specific clinical features which are drusens and changes in RPE layers. A higher stage of AMD depends on the damage of vision. A clear difference in the central vision of normal and diseased (AMD) eye can be seen from the figure 2.6(a) and 2.6 (b) [4].

**Figure 2.6(a)Normal Eye Vision [11]** **(b) Diseased (ARMD) Eye Vision[11]**

In developed countries most of the people who are 50 years old or above suffers from aged related macular degeneration. It affects 10% of people whose age is greater than or equal to 65 and 25% of those people whose age is greater than 75 years. In only United States almost 10

million people are suffering from this disease and this number is projected to be increased by 50% up till 2020 [13][14].

In the natural course of the human aging process retina also undergoes some major changes. These changes sometime appear as polymorphous debris,a yellow decomposition of a cell which is visibly ophthalmoscopically known as drusens. Drusens are formed between Bruch's membrane and retinal pigment epithelium (RPE). Drusens are characterized on the basis of their sizes as small (drusens having a diameter less than 63mm), medium (diameter that ranges between 63mm and 124mm) or large (diameter that is greater than 125mm).

Drusens are the main characteristic feature, or physical sign of age related macular degeneration. People having small drusens with no other abnormalities present have fewer chances to develop advanced age related macular degeneration. In advanced AMD one should also have from following abnormalities:

- Retinal pigment epithelium focal detachment.
- Growth of new blood vessels between Bruch's membrane and retina.
- Lesions (Outer Retinal atrophy) that causes loss of central vision that involves choroidal neovascularization (CNV).

In aged related macular degeneration a wide range of clinical characteristics is shown by patients that vary from drusen sizes to different AMD abnormalities [11].

#### 2.4.1.1 Types of AMD

1. Usually AMD is divided into two major types:

**a Dry (non-exudative) AMD**

The most common form, this type of AMD can be easily diagnosed and its diagnosing ratio is 90%. The advanced stage of dry AMD is geographic atrophy (GA). This disease, even in its advanced stage is less able to cause vision loss.

**b Wet (exudative) AMD**

It is considerably less common than dry AMD. This type of AMD is more linked to rapid progress towards advanced vision loss. The main characteristics or features of this type of AMD are (CNV) and pigment epithelial detachment (PED).

### 2.4.1.2 Wet (exudative) AMD

This is a prolonged eye disease which at the center of your vision causes vision loss. This disease is caused by the abnormal vessels of blood that leaks blood and fluid into the region of the macula or due to detachment of retinal pigment [12]. The advancement in wet age related macular degeneration is shown in figure 2.7.

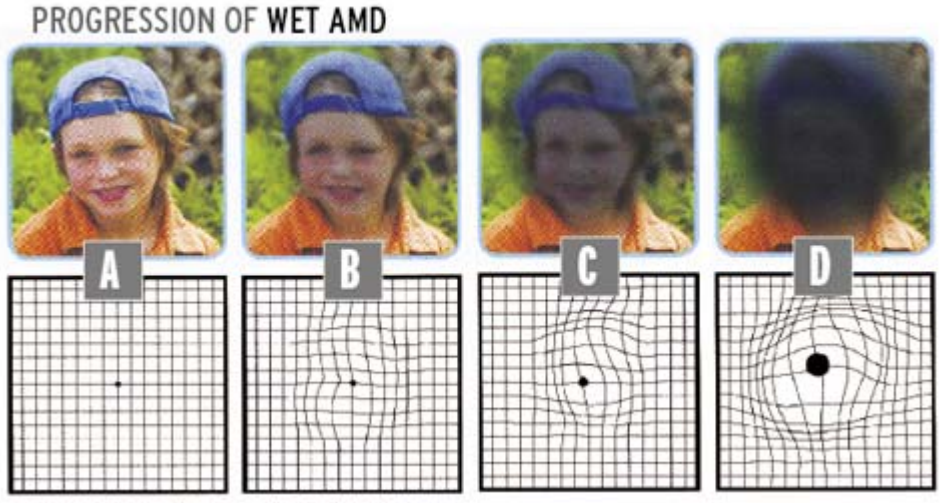


**Figure 2.7 Moving from normal vision (A) to Wet AMD (D) [10]**

### 2.4.1.3 Eye Tests and Examination

When you undergo the process of eye examination some drops must be put into your eyes. These drops are used to dilate your pupils. After that the doctor will view your optic nerve, blood vessels and retina using special lenses.

In macular disorders the doctor will look for specific macular changes. In case of Wet AMD they will look for CNV and RPE. During your eye examination you can be asked to cover your eyes one by one and to observe the line patterns. These line patterns are called Amsler Grid. You will be suffering from AMD if the straight line appears wavy to you. The wavier the line, advances is the level of Wet AMD (figure 2.7).Other tests that may be referred by the doctor to you include:

- Optical Coherence Tomography (OCT).
- Fluorescein Angiogram.
- Fundus Photography.

### a Fundus photography

Fluorescein angiography uses cameras and a special dye to monitor blood flow in the two layers present on the back of the eye known as the choroid and retina [15].

### b Fundus photography

Fundus photography which is commonly known as fundography is a sort of camera that creates a photograph of the eye's interior surface. This surface includes optic disk, retina, fundus (i.e. Posterior pole) and macula.

Fundus photography is widely used by medically trained professionals, ophthalmologists, optometrists to perform following listed functions [15].

- To closely monitor the disease progression.
- Disease Diagnosis.
- Epidemiology.

### c Optical coherence tomography (OCT)

It is a renowned and established medical imaging technique. It is used in various fields of life. Some major uses of OCT are discussed ahead.

- **Use of OCT in Ophthalmology**

This technique is extensively used by the ophthalmlogist in order to get images of higher resolution of the anterior segment of eye, retina, macular degeneration [17] and direct method to asses multiple sclerosis of axonal integrity [16].

According to researchers it's also a reliable and important tool to observe glaucoma progression [18].

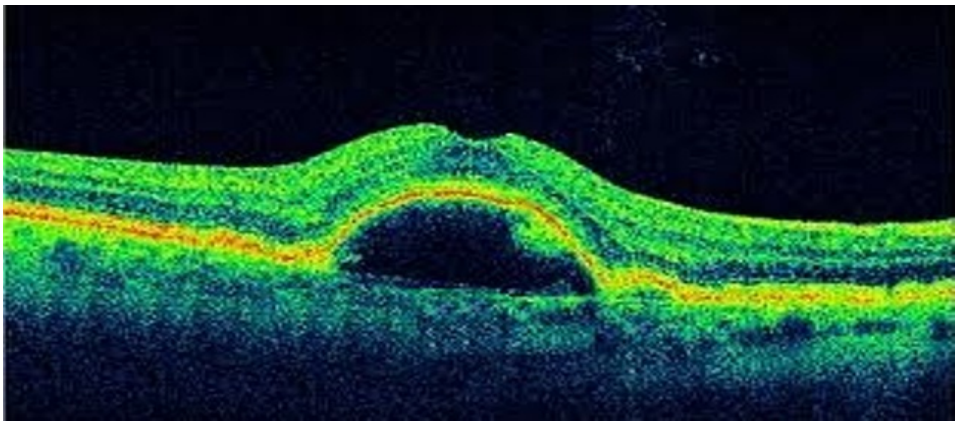

**Figure 2.8 OCT image of Eye Suffering from Wet ARMD (having PED) [4]**

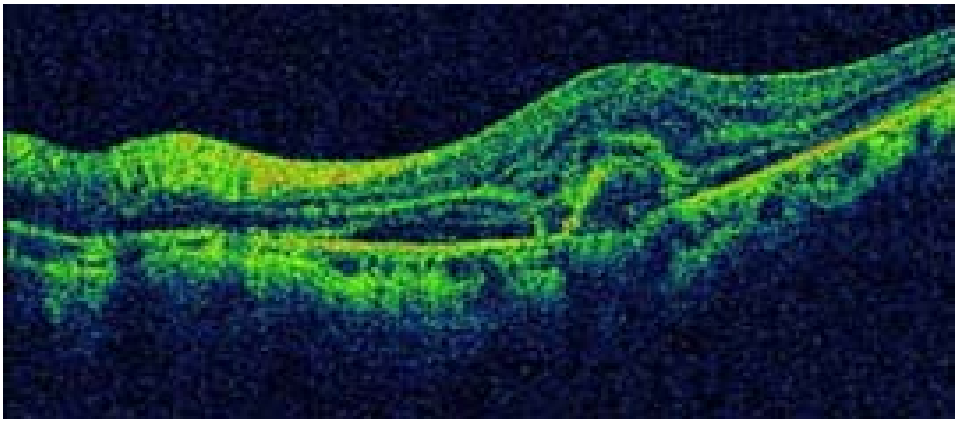

**Figure 2.9 OCT image of Eye Suffering from Wet ARMD (having PED and CNV)**

- **Use of OCT in field of Neurology and Cardiology**

Researchers are very keen to invent such methods that will use OCT (frequency domain) which will take picture of coronary arteries to in order to detect vulnerable lipid rich plaques.

Researchers are using OCT imaging techniques to get detailed mice brain images. The image will be taken through "window" which is made from Zirconia. That window has to be modified and to be implanted in the skull transparently. [18]

- **Use of OCT in industry**

Optical coherence tomography, these days are getting very applicable and it is increasingly used in industrial applications like:

- Material Thickness Measurements [19].
- Volume loss measurements.
- Surface and cross-section imaging [25].
- Particular thin silicon wafers [20][21].
- Compound Semiconductor wafers thickness measurements [22][23].
- Non Destructive Testing (NDT) [19].
- Surface roughness characterization [24].

The OCT system having feedback is able to control the manufacturing process present in industries [26]. In-line and off-line task can be achieved using OCT having sub-micron resolution and high speed data acquisition [27].

OCT systems that are based on fiber are mostly more flexible to the industrial environment [28]. These systems can scan and access hard to reach space interiors and are capable to perform operations in unfriendly environments which are whether cryogenic, very hot or radioactive [29] [30].

These three are the most common test that is referred by the ophthalmologist in order to detect any sort of macular disorder.

### 2.4.2 Age-related Macular Hole

This disease causes is the most common one which causes the loss of a person's central vision. Research surveys have found that 3 out of 1000 individuals suffer from this disease. The occurrence of this disease is at its peak in females over the last $7^{th}$ decades. The major cause of this disease is Antero-posterior traction, tangential traction and abnormal vitreofoveolar attachment. An example of the Aged related macular hole is shown in figure 2.10 (fundus image, OCT image).

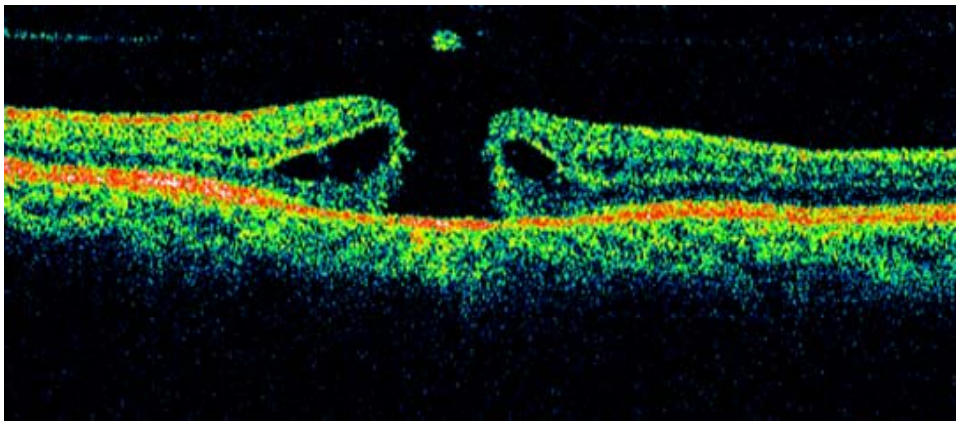

**Figure 2.10(a) OCT image of eye suffering from Macular Hole [5]**

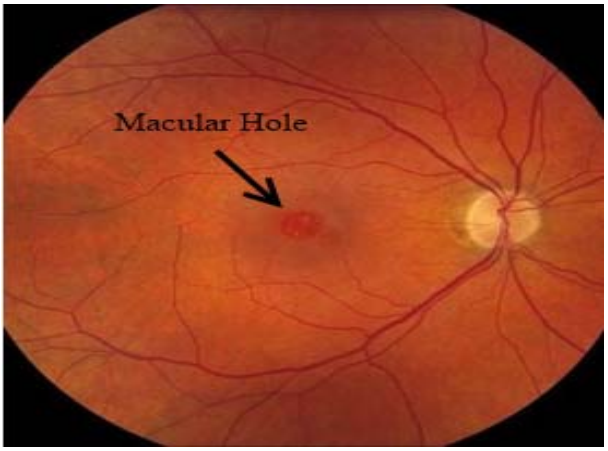


**Figure 2.10(b) Fundus Image of Eye with Macular Hole [5]**

### 2.4.3 Polypoidal Choroidal Vasculopathy

This is an idiopathic choroidal vascular disease which is usually referred to as posterior uveal bleeding syndrome (shown in figure 2.11). PVC is normally characterized by a wide network of inner choroidal vessels with multiple terminal aneurysmal protuberances. The occurrence of this disease is most common in East Asian and African ethnic origin patients. Surveys have also concluded that this disease is more common in women than in men and the ration of it is 5:1. The disease is normally present in both eyes, i.e. bilateral in normal cases but in case of severity,it is asymmetrical. Fundus image of eye suffering from polypoidal choroidal vasculopathy is shown in figure 2.11.

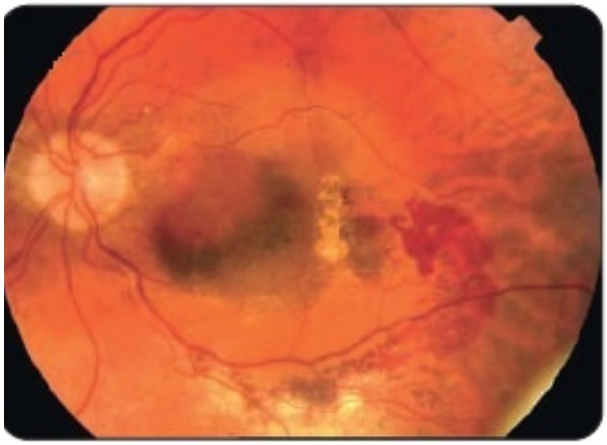

**Figure 2.11 Fundus image of Eye having Polypoidal choroidal vasculopathy [6]**

### 2.4.4 Central Serous Retinopathy

Central serous chorioretinopathy (CSCR) is an idiopathic disorder (shown in figure 2.12 a&b), the pathogenesis of this disease includes:

- Serious detachment (Localized) at the macula of sensory retinal.
- Leakage from the choriocapillaris through focal, or, less commonly diffuse, hyperpermeable RPE defects.

CSCR usually affects one eye of a Caucasian middle-aged or young man. Most women that suffer from CSCR are older. Additional risk factors include pregnancy, steroid

administration;type a personality, Cushing syndrome, psychological stress, systemic lupus erythematosus, and steroid administration.

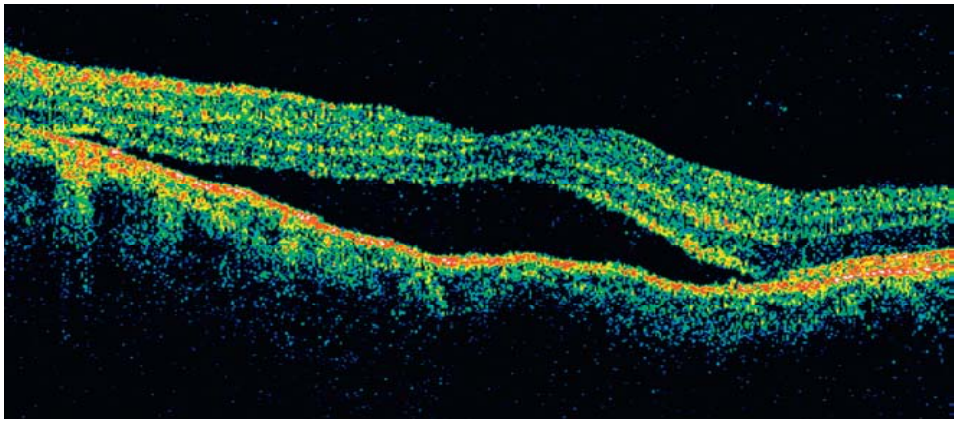

**Figure 2.12 (a) OCT image of Eye having Central serous chorioretinopathy [5]**

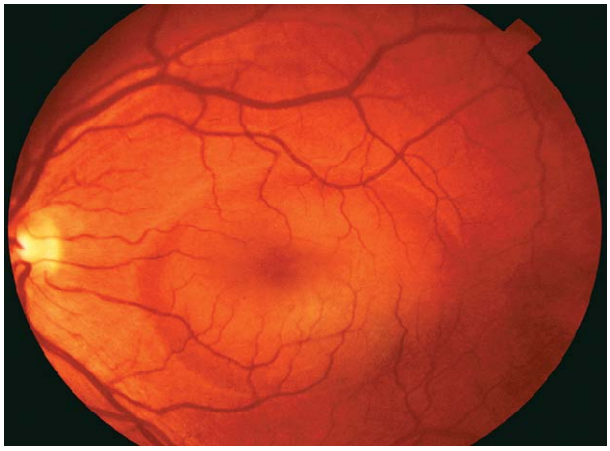

**Figure 2.12 (b) Fundus image of Eye having Central serous chorioretinopathy [5]**

### 2.4.5 Cystoid Macular Oedema

Cystoid macular oedema (CMO) results from inner nuclear layers of the retina with the formation of cyst-like changes and the accumulation of fluid in the outer plexiform (shown in figure 2.13 a &b). Initially the fluid, with subsequent rupture, may start to gather intracellularly in Müller cells. In case of long-standing the larger cavities will be formed by the combination of smaller microcystic spaces. This may advance towards the lamellar hole formed in the fovea with permanent damage of central vision. CMO is a particular manifestation of some sort of

maclar oedema. OCT image and fundus image of eye suffering from CMO is shown in figure 2.13 a, b.

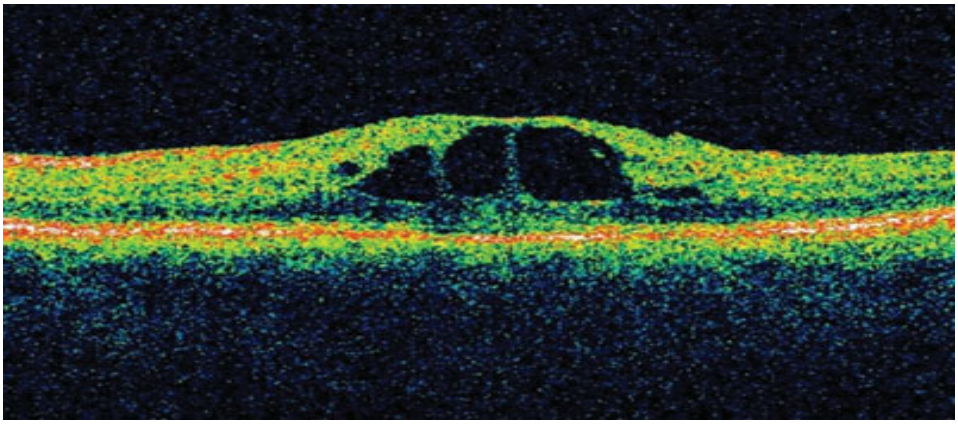

**Figure 2.13 (a)** **OCT image of eye suffering from Cystoid macular oedema [5]**

**Figure 2.13 (b)** **Fundus image of eye suffering from Cystoid macular oedema [5]**

### 2.4.6 Macular Epiretinal Membrane

An epimacular membrane (EMM), also called as macular pucker, macular epiretinal membrane and cellophane maculopathy. EMM is a fibrocellular structure like sheet that develops on or above the retinal surface. Cellular components proliferation and membrane contraction cause visual symptoms, mainly because of wrinkling of the retina, localized and obstruction with or without CMO. The OCT image and fundus image of EMM are shown below in figure 2.14 a, b.

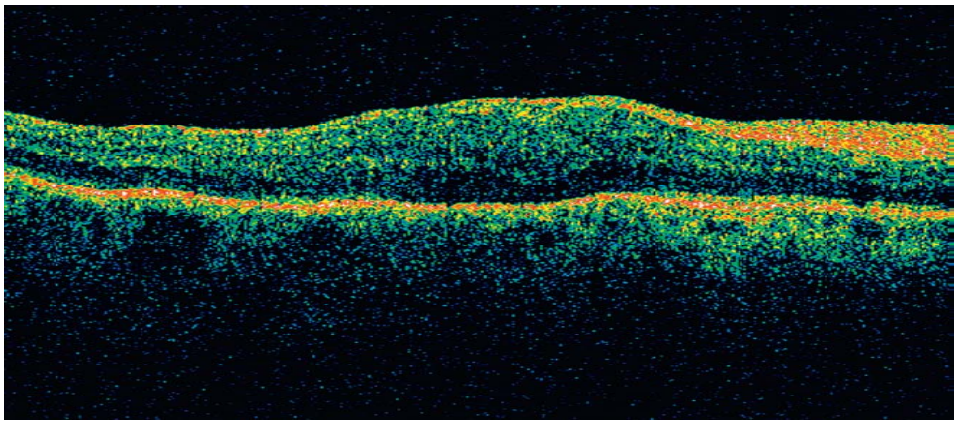

**Figure 2.14 (a)** **OCT image of eye suffering from Macular Epimacular Membrane [6]**

**Figure 2.14 (b)** **Fundus image of eye suffering from Macular Epimacular Membrane [6]**

### 2.4.7 Degenerative Myopia

Myopia is caused due to environmental factor and as a result of the complex the result of complex hereditary. When there is a refractive error of more than -6 diptres, its high myopia. In high myopia axial length is typically greater than 26 mm (shown in figure 2.15).

Degenerative or 'Pathological' is caused by scleral enveloped progressive anteroposterior elongation that is linked with a range of secondary ocular changes, it is a principal thought which linked it to the mechanical stretching of the involved tissues. It is the main cause of vision loss and most legal cause of blindness.

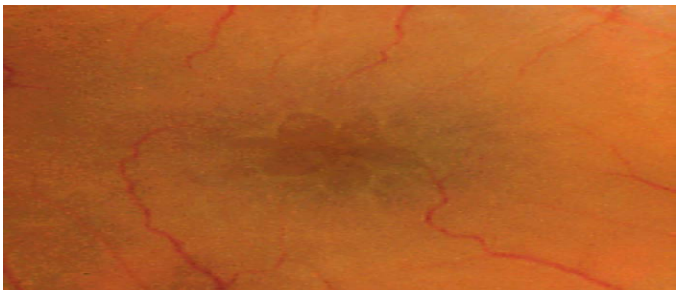

**Figure 2.15 Fundus image of eye suffering from Degenerative Myopia [5]**

### 2.4.8 Angioid Streaks

Angioid streaks are crack-like dehiscences in brittle thickened and calcified Bruch membrane, associated with atrophy of the overlying RPE.

### 2.4.9 Choroidal Folds

Choroidal folds are parallel grooves or striate involving the inner choroid, Bruch membrane, the RPE and sometimes the retina (chorioretinal folds). This disease develops its association in any process that persuades sufficient compressive stress within the Bruch membrane, choroid and retina. Primary mechanisms include choroidal congestion and scleral compression, and occasionally tissue contraction. Choroidal folds should be distinguished from retinal folds, which have a different pathogenesis (usually epimacular membrane). Fundus image of eye suffering from choroidal folds is shown in figure 2.16.

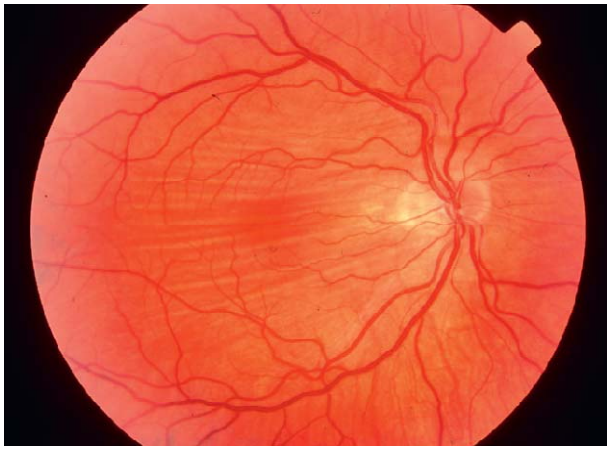

**Figure 2.16 Fundus image of eye suffering from Choroidal folds [6]**

### 2.4.10 Hypotony Maculopathy

Eyes developing Hyptony commonly have Maculopathy (shown in figure 2.17). It is defined as IOP less than 5mmHg. The major cause of this disease is the excessive drainage which is followed by the glaucoma filtration surgery (With adjunctive antimetabolite risks are higher). Some other causes include:

- Trauma either caused by penetrating injury or by cyclodialysis cleft.
- Chronic uveitis occurred due to tractional ciliary body detachment caused by cyclitic membrane and by direct impairment of ciliary body function, and retinal detachment.
- Hypotony may be eternizing due to the development of secondary choroidal effusion. Hypotonous with the passage of time can itself cause further damage, which includes atrophy of ciliary and sclerosis process. Hypotony that prolonged lead to complete loss of eye or phthisis.
- The only treatment is to restore the normal IOP.

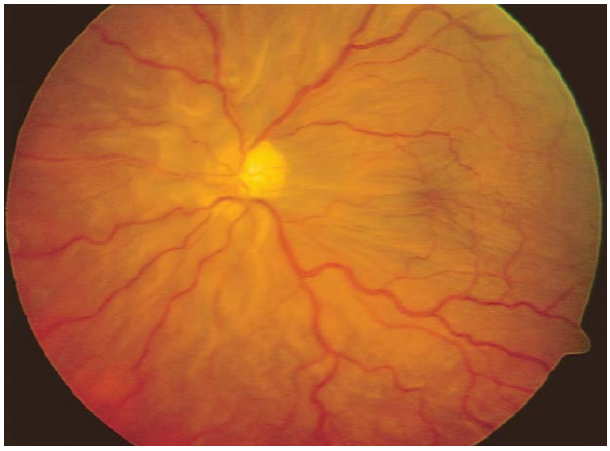

**Figure 2.17 Fundus image of eye suffereing from Hyptony Maculopathy[6]**

### 2.4.11 Vitreomacular Traction Syndrome

In vitreomacular traction syndrome (VMT), the vitreous cortex is detached from the perifoveal region and but remains attached to the fovea, this may result in exertion on fovea by persistent anteroposterior traction. In VMT most of the changes at the retina and posterior hyaloid membrane are similar to the those that occurred in the macular hole formation and in the EMM.

### 2.4.12 Solar Maculopathy

Solar Maculopathy is a retinal injury also known as eclipse retinopathy. This disease is caused by the photochemical effects present in the solar radiation, which are exposed to the eye when a person directly or indirectly views the sun.

### 2.4.13 Idiopathic Choroidal Neovascularization

Idiopathic CNV is an uncommon condition which affects patients under the age of 50 years and is usually unilateral. The diagnosis is one of exclusion of other possible associations of CNV in younger patients such as angioid streaks, high myopia and chorioretinal inflammatory conditions such as presumed ocular histoplasmosis, MEWDS or PIC. The condition carries a better visual prognosis than that associated with AMD and in some cases spontaneous resolution may occur. The CNV lies predominantly above the RPE (type 2), is often encircled by reactive RPE growth. PDT has met with variable results, but anti- VEGF agents show promise.

## 2.5 Summary

Our main concern was the detection of wet aged related macular degeneration; literature review and proposed methodology along with the achieved results are discussed in the chapters ahead.

# CHAPTER 3 LITERATURE REVIEW

Wet aged related macular detection using image processing techniques can be classified into basic steps like noise removal from OCT images, segmentation of the abnormalities related to the disease, feature extraction and then classification. Most of the system designed and the research work performed for the detection of wet aged related macular degeneration is usually done using fundus images, but now as every ophthalmologist prefers optical coherence tomographic test to detect various diseases, this increases the need of research work to be performed using OCT images. OCT test in ophthalmology is considered more advanced and reliable source as these images provide the in depth view of retinal layers. Previous research work performed for the detection of wet aged related macular degeneration and on OCT images is summarized in this chapter.

## 3.1 Aged Related Macular Degeneration Detection using Fundus images

Detection of age related macular degeneration using fundus images is mostly done by detection the presence of drusens in the macula. The type of age related macular degeneration is then classified by the type of drusens. Automated drusens detection is done in fundus images. Yuanjie et al [31] presented an approach that detects drusens by using color fundus images. The system proposed by them uses a learning based drusen detection technique. The main goal behind their system design was to automatically access his risk of development of ARMD. The technique used incorporates image denoising and image analysis for fundus images, illumination correction and color transfer. Their work was different than the previous work as it includes robust multiscale local image descriptors and optimal color descriptors in the process of drusen detection. The system performance was evaluated on the bases of two AMD clinical studies**.** The system designed proved to be the state of the art system. FAF images are widely used in the diagnosis of ARMD.

Macular Degeneration is the leading cause of blindness in people over 55. There are two kinds of AMD: wet and dry. The most common is the dry form. It is characterized by atrophies of the retinal pigment epithelium (RPE) with subsequent photoreceptor degeneration. The atrophy severity depends on its size and its location with regard to fovea. The fovea is the macula center, which is the retina central zone (about 2mm of diameter). The macula has a high density of cone photoreceptors and is not supplied by the retinal capillaries; it receives its blood supply from the choroid. For the determination of the lesions location, A. Rashid et al [32] developed an automatic positioning and orientation of a retinal grading grid. Centered on the fovea, it provides information on the spatial distribution of pathologies and thus helps to determine the severity and the danger associated with the detected retinal lesions.

Carla Agurto et al.[33] used digital retinal photographs to detect the presence of pathologies that are relevant for aged related macular degeneration and diabetic retinopathy. The pathologies include; hemorrhages, microaneurysms, exudates, neovascularization in the optic disc and elsewhere, geographic atrophy, abnormal pigmentation and drusens. The system algorithm was based on detecting the presence or absence of the pathologies. Different values of sensitivity and specificity are achieved after applying threshold and a Receiver Operating Characteristic Curve is constructed.

Alauddin Bhuiyan et al. [34] used different Local intensity distribution, adaptive intensity thresholding and edge information to detect potential drusens area. The author has considered 50 images in order to detect different type of drusens. To perform segmentation of drusens 12 images was selected and expert grader marked the drusen region in pixel level. Quantified area is calculated with sensitivity and specificity by performing a comparison of drusen detects output images with the hand labeled images.

Teleophthalmology has a great potential which improves the access, quality and affordability of health care. D.Jayanthi et al. [35], used teleophthalmology for patients reduces the need for travel and super-specialist. The purposed system diagnosis the presence of drusens in the retina using a neural network based classifier.

## 3.2 Noise Removal in OCT images

Speckle noise is a sort of granular noise that inherently exists in and degrades the quality of coherent imaging devices. It is also the major problem in OCT images, as it lowers resolution and contrast. To deal with this problem numerous techniques are developed.

Prakash Duraisamy et al [36] provided two approaches one subjective and other objective, to enhance the contrast of OCT images. Tao Liu et al. [37] presented an approach that reduces the speckle noise using wavelet reconstruction and decomposition. The results show the algorithms improve the image contrast without losing the sharpness.

Vikas Gupta et al. [38] Proposed a computerized automation method based on wavelet denoising to reduce speckle noise from OCT images. In order to computerize the parameters used in wavelet transform an evolutionary methodology is used known as Differential Evolution. This method improves the signal to noise ratio (SNR) to 17%. Aside from wavelets, homomorphic Wiener filters discussed by G. Franceschetti et al. [39] and adaptive mean filter discussed by J.M.Schmitt et al. [40] were also used to remove granular noise (Speckle Noise).

## 3.3 Segmentation of Retinal Layers in OCT images

The second most important research was regarding OCT images is the segmentation of retinal layers.

Tapio Fabritius et al. [41] developed the segmentation techniques to segment the retinal layers present in the OCT of an eye, his methodology was based on a variation of signal intensity. His aim was to reduce the calculation time. Mainly two algorithms were developed; one was used for identifying internal limiting membrane, the second was used to identify retinal pigment epithelium. These algorithms were used to estimate the structural features of the retina. The main ambition of this algorithm was to reduce the required calculation time.

D. Cabrera Fernández et al. [42]showed that with the help of local coherence information about the retinal structure, retinal layers can be located interactively and automatically with good accuracy. Optical coherence tomographic images are processed with techniques like texture

analysis combined with complex diffusion filtering**.** OCT images are processed using the ideas of texture analysis by means of the structure tensor combined with complex diffusion filtering. Using this methodology the system has achieved good performance in removing speckle noise from the images, enhancing and segmenting the layers of the retina.

S. Chiuet al. [43]automated the segmentation of retinal layers present in OCT images using dynamic programming and graph theory. The results obtained from this technique accurately segment the boundaries of eight retinal layers. But this approach has a drawback as it can only segments the retinal layers of normal adult eyes.

Qing Dai in [44]presented a segmentation technique which segments the six intra-retinal boundaries in OCT images. This algorithm consists of four main steps, firstly the images will be filtered using bilateral filter, in second step image is broken into numerous non-vessel sections in accordance to the retinal blood vessels. In the third step gradient information is used to segment different layers and in the last step the optimization of edge selection is done using shortest path search. This algorithm was also validated with manual segmentation and it shows high accuracy. But this algorithm only performs segmentation on normal OCT images. A. Mishra et al. [45] gives extension to tradition active contour schemes by using two-step kernel-based optimization scheme.

## 3.4 Wet Aged Related Macular Degeneration Detection using OCT images

Very little research work is done in the detection of wet aged related macular degeneration using optical coherence tomographic images. The methods and techniques used by the authors are described below:

PA. Dufourin [46],a method is builtby the author to classify between age related macular degeneration and healthy eyes. A statistical shape model is built from the population of healthy eyes having a close fit in healthy regions. This model does not fit when certain morphological abnormalities are present in the segmented regions. Fitted error is calculated from this model and

visualization of pathologies can be done very quickly. This model will locate the presence of drusens in the RPE layer.

Another approach developed by Sun Young Lee et al. [47] detects PEDs in Oct images using software algorithm and achieved the specificity and sensitivity of 84% and 81.67%.

Anam Haq et al. [48] used morphological operations to detect abnormalities in optical coherence tomographic images that are associated with wet aged related macular degeneration. The proposed system statistical measures are calculated which includes accuracy, sensitivity, and specificity. The designed system achieved the sensitivity and specificity of 95% and 93.55%.

# CHAPTER 4 SYSTEM DESIGN

## 4.1 Proposed Methodology

Through the automatic detection of PED and CNV we can be able detect wet AMD early and can save patients' vision. In order to achieve such automation it is therefore necessary to design a computer aided system. We have to design a system which operates on a dataset consisting of 51 OCT images. Out of these 51 images 21 images contain Wet AMD images and 30 are the OCT images of healthy patients. The system design developed by us consists of four main blocks. The results obtained through each step of processing are shown along with their description.

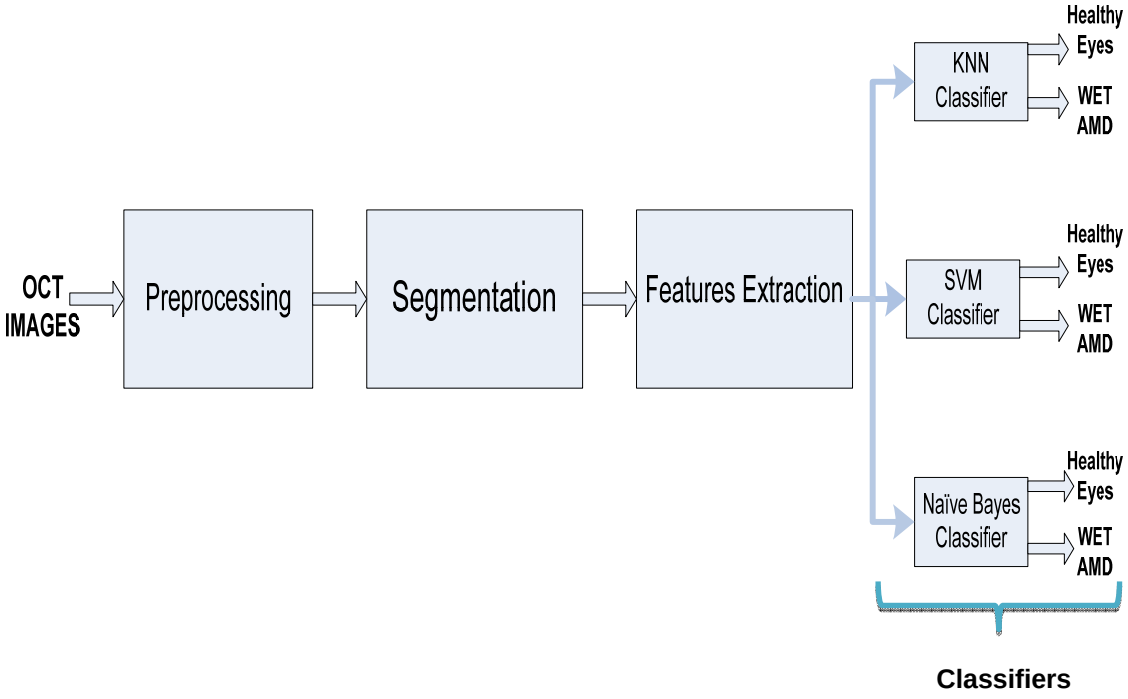


**Figure 4.1 Flow Diagram of Designed System**

## 4.2 Preprocessing

The preprocessing block consists of two sub blocks which are “filtering” and “roi extraction”. The flowchart of the preprocessing block is shown below in figure 4.2.

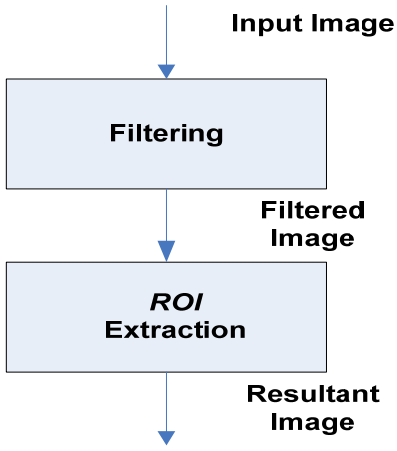


**Figure 4.2 Flowchart of Preprocessing Block**

### 4.2.1 Noise Removal

OCT Images from the dataset consists of speckle noise. This noise is removed from the image by filtering. We have used a median filter to remove speckle noise from the OCT images. Median filter of *wxw* window is designed;

$$\hat{k}(x,y) = median_{(m',n')\in D_{xy}}\{h(m',n')\} \quad (4.1)$$

In above equation x and y are the filtered image coordinates, h is the original image and m’ and n’ are the coordinates of the sub image D. A filter of mask 3x3 is used in the system.

### 4.3.2 Region of Interest Extraction

After performing the noise removal region of interest (ROI) is extracted from the resultant image.Abnormalities like PED and CNV are present near the RPE layer. So the same region above and below RPE is extracted in this technique.

The result of preprocessing is shown below in figure 4.3b, along with the original image shown in figure 4.3a.

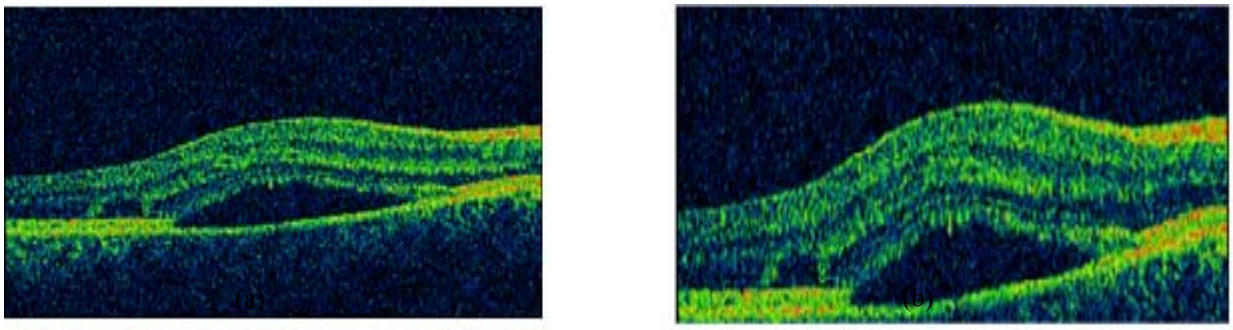

(a) (b)

**Figure 4.3 a) Original Wet AMD Images. b) Preprocessed Image.**

## 4.3 Segmentation of PED and CNV

To segment the pathological abnormalities like PED and CNV from the image we have performed segmentation of OCT images. This segmentation is done in two steps. In step 1 color based segmentation [49] is performed and in step 2 morphological operations [50] are used to detect these abnormalities. Figure 4.4 shows the flowchart of segmentation block.

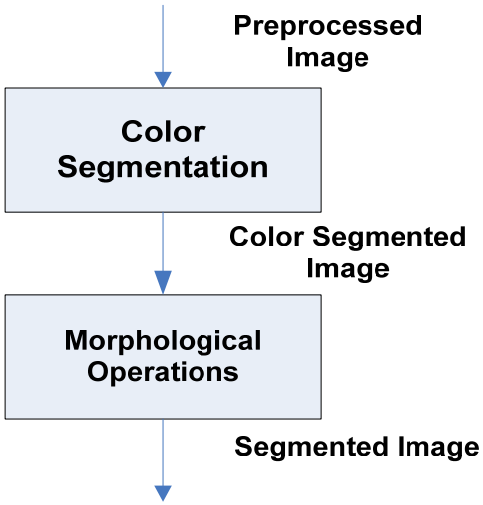


**Figure 4.4 Flowchart of Segmentation Block**

### 4.3.1 Color Segmentation using K-mean Clustering Algorithm

To segment images there are a variety of different segmentation techniques available. These techniques can be differentiated on the basis of concepts like contour, pixel orientation, region, and color. Out of these, color segmentation is the most crucial one and is used in many industrial fields like medicine, remote sensing, etc. color segmentation performance can significantly affect the image quality [49].

#### 4.3.1.1 K-mean Clustering

K-mean uses unsupervised learning approach to classify data into clusters. It determines the spectral grouping present in the dataset. The algorithm first accepts the number of clusters it needs to create from the user which in our case is three, as three main colors are present in OCT images. It then starts an arbitrary locating the number of cluster centers. After locating the cluster centers each image pixel is allocated to the cluster whose mean distance is a closet in cluster center. Class mean is calculated after allocating pixel points to the cluster. The algorithm repeats itself until there is no change in the class mean. These are the major steps use in color based segmentation of OCT images [49].

Following are the steps of performing Color Segmentation using K mean clustering:

| |
|---|
| **1. Load/Read image.** |
| **2. Decoration is applied for color separation.** |
| **3. The image is converted to L*a*b color space from RGB Color space.** |
| **4. Classify the image obtained from step 3 using k-mean clustering.** |
| **5. Label the image pixels obtained from step 4.** |
| **6. Create the images which are segmented by color.** |

## 4.3.2 Morphological operations

There are four basic operations in morphology. These operations are dilation, erosion, opening and closing. These operations have their own features in gray scale images and binary images [50]. A series of morphological operations are performed on OCT images in order to extract the pathological abnormalities (PED and CNV).

### 4.3.2.1 Dilation

This morphological operation basically thickens the binary image. The size or amount of thickening is controlled by the structuring element. This structuring element can be of different sizes and shape.

$$\boldsymbol{I} \oplus \boldsymbol{S} = \{\boldsymbol{z} | [(\widehat{\boldsymbol{S}})_{\boldsymbol{z}} \cap \boldsymbol{I}] \subseteq \boldsymbol{I}\} \qquad (4.2)$$

In the above equation "*I*" is the image and S is the structuring element that is viewed as a convolution mask [49] [50].

### 4.3.2.4 Erosion

This operation thins or shrinks the objects present in a binary image. Mostly erosion is viewed as a filtering operation as it removes the small details of an image. Similar to dilation erosion is also controlled by the structuring elements which can have different shapes and sizes [49] [50].

$$I \oplus S = \{z | (\widehat{S})_z \subseteq I\} \qquad (4.3)$$

The other two operation *opening* and *closing* used by us are the combination of dilation and erosion.

#### 4.3.2.4 Opening

Opening normally smooth's the object contour; break the narrow discontinuities and takes out the thin protrusions. The opening of image $I$ with structuring element $S$ is denoted by $I \circ S$.

$$I \circ S = (I \ominus S) \oplus S \qquad (4.4)$$

This equation shows that opening of $I$ by $S$ is erosion followed by dilation [49] [50].

#### 4.3.2.4 Closing

Similar to opening closing operation smooth's the contour, but opposite to opening it joined together the narrow gaps and hollows between object, it also fills the gaps and remove the small holes from the image. The closing operation on an image $I$ with structuring element S is represented by $I \cdot S$ .

$$I \cdot S = (I \oplus S) \ominus S \qquad (4.5)$$

This equation says the closing is simply the dilation of $I$ with $S$ followed by erosion. We have performed all these operations in our simulation. The dilation is performed by a different structuring element greater in size as compared to the structuring element by which the image is eroded [49] [50] [51].

After performing the morphological operation, labeling of connected component is performed and undesired labeled objects are eliminated from the image. Results which are obtained after segmentation is shown in figure 4.5 a,b.

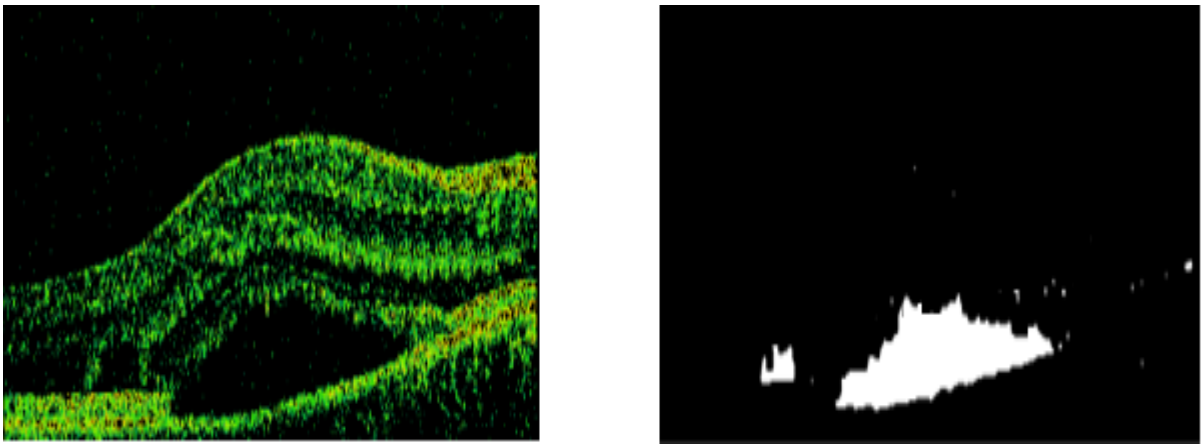

(a) (b)

**Figure 4.5 a) Colour Segmentation using k-mean clustering. b) PED and CNV detection using Morphological Operations.**

## 4.4 Feature Extraction

A total of eight features are extracted after segmenting CNV and PED from the images. A feature vector {$f_1$, $f2$, $f_3$, $f_4$, $f_5$, $f_6$, $f_7$, $f_8$} is created for each image in the dataset. These features include Area, Orientation, Eccentricity, Minor axis length, Major axis length, Equivalent Diameter, Mean intensity and Maximum Intensity. Flowchart of feature extraction block is shown below in figure 4.6.

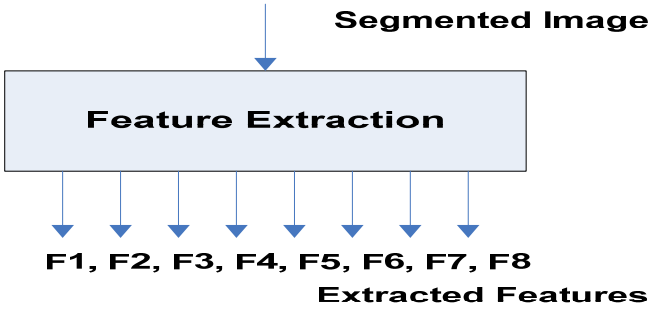


**Figure 4.6 Flowchart of Feature Extraction**

**The description of these features is given below:**

1. ***Area ($f_1$)*:** It is defined as the total number of pixels present in the filled region.
2. ***Orientation ($f_2$)*:** Is defined as the angle between the horizontal axis and the major axis of the ellipse.
3. ***Eccentricity ($f_3$):***Is the eccentricity of the ellipse which has the same second moments as the region. It is the distance ratio between the foci and the major axis of the ellipse. The range of this parameter varies between 0 and 1. (The ellipse having 0 is actually a circle and ellipse having 1 is a line segment)
4. ***Equivalent-Diameter ($f_4$):*** Specifies the circle's diameter with the same value of the area as a region. It is calculated using the following formula:

$$EquiDiameter = \sqrt{\frac{4*Area}{pi}} \qquad (4.6)$$

5. ***Major-axis-length ($f_5$):***Specifies the length of ellipse major axis, which has the same normalized second central moments as the region**.**
6. ***Minor-axis-length ($f_6$):***Specifies the length of ellipse minor axis, which has the same normalized second central moments as the regions.
7. ***Maximum Intensity ($f_7$):*** It's the maximum pixel intensity in the region.
8. ***Mean Intensity ($f_8$):*** It's the mean value of the pixel intensities present in a given region.

These feature vectors are passed to the classifiers in order to perform detection between Wet AMD and healthy eyes.

## 4.5 Classification of Wet Aged Related Macular Degeneration

To classify between Wet AMD and healthy patients the created feature vectors are passed to the classifiers. In final classification supervised learning approach is used, i.e. dividing the data set into two portions training data set and testing data set. We have defined two classes, $C_1$ and $C_0$, $C_1$ corresponds to Wet AMD and $C_0$ denotes healthy eyes. From this class information a labeling

vector of size mx1 is created. This labeled vector is also passed to the classifier during the training process. A Flowchart of classification block is shown in figure 4.7 below:

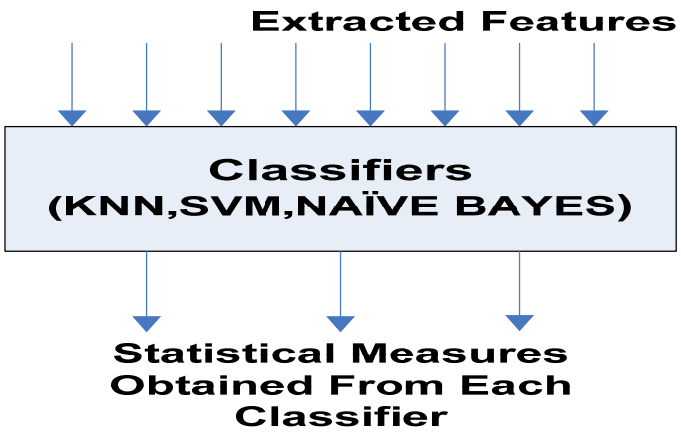


**Figure 4.7 Flowchart of Classification block**

We have used three classifiers in the detection process. These classifiers are

1. **K-nearest Neighbor.**
2. **Naïve Bayes.**
3. **Support Vector Machine.**

### 4.4.1 K-Nearest Neighbor classifier

This algorithm is one of the simplest among all machine learning algorithms. K-nearest neighbor performs classification on the base of closest training samples in the features space. In training this algorithm only stores the feature vectors with the labels of training images. In testing process the unlabeled test sample is assigned the label of the nearest neighbor. Nearest Neighbor is calculated using Euclidean distance. The formula for Euclidean distance is given below

$$\boldsymbol{dist}(\boldsymbol{x},\boldsymbol{y}) = \left|\left|\boldsymbol{x}-\boldsymbol{y}\right|\right| = \sqrt{(\boldsymbol{x}-\boldsymbol{y}).(\boldsymbol{x}-\boldsymbol{y})} = (\sum_{\boldsymbol{i}=\boldsymbol{1}}^{\boldsymbol{m}}(((\boldsymbol{x_i}-\boldsymbol{y_i})^{\boldsymbol{2}}))^{\boldsymbol{1/2}} \qquad (4.7)$$

Most commonly the test sample is classified based on the labels of its k-nearest neighbor [54]. If the value of k=1 then in that case k-nearest neighbor is equal to the nearest neighbor algorithm.

In cases where we have to distinguish between two classes, it's better to use odd values of k [52] [53].

In our system we have considered the value of k from 1 to 12. We have calculated accuracy against each value of k and then the final accuracy is defined as a mean value of these accuracies.

Following are the steps that are followed in the classification process:

| |
|---|
| **1. The feature vector is first shuffled and divided into 4 folds.** |
| **2. For each fold, i.e. from a to d:** |
| **a. The value of k is varied from 1 to12** |
| **b. The classifier is trained on each fold's training data set.** |
| **c. The test sample/features from each fold are passed to the classifier.** |
| **d. Euclidean distance is calculated for each feature.** |
| **3. The test sample is assigned the label of the class which is closer to it.** |
| **4. Accuracy is calculated against each value of k.** |
| **5. The accuracy of each fold is calculated.** |
| **6. Mean accuracy is calculated by using the formula:** |
| $\textbf{Mean Accuracy} = \frac{\textbf{TotalAccuracy}}{\textbf{Total number of folds}}$ **(4.8)** |

## 4.4.2 Support Vector Machine

SVM uses the supervised learning model. This model divides data points using different planes in space [54]. Normally SVM takes a set of data points and predict that out of the two classes they belong to which class. This is often known as probabilistic binary linear classifiers [56] [57]. It uses optimum linear hyper planes in order to separate the two sets of data in a given feature space. This kind of optimum hyper plane is obtained by maximizing minimum margin between the two sets; the hyper plane produced as a result will be only dependent on border training patterns called support vectors [55].

The formula used in the classification of test samples/features in our system is mentioned below:

$$\boldsymbol{c = \sum_i \alpha_i k(s_i, x) + b} \qquad \textit{(4.9)}$$

$$\begin{cases} if\ c \geq 0\ test\ sample\ belong\ to\ C_0 \\ if\ c < 0\ the\ test\ sample\ belong\ \ to\ C_1 \end{cases}$$

$S_i$ in the above formula is the support vectors. $\alpha_i$ are the weights, b is the bias and k is the kernel function. In linear svm k is the dot product.

### 4.4.3 Naive Bayes Classifier:

Naïve bayes classifier is a probabilistic classifier based on Bayes' theorem [60]. This classifier considers every feature to contribute independently to the probability, irrespective of the presence and absence of other features. As naïve classifier follows the bayes theorem to assign the most likely classes to a given sample mentioned in its feature set. Aside from this unrealistic assumption, naïve bayes is remarkably successful as compared to other sophisticated classifiers [58].

$$\boldsymbol{P(C|X_i) = \frac{P(C).P(X_i|C)}{P(X)}} \qquad \textit{(4.10)}$$

In the above equation$P(C|X_i)$ is known as the posterior probability, $P(X_i|C)$ is the class conditional probability,$P(C)$ is prior probability and $P(X)$ is the total probability of the system.

Following are the steps of classification using Naïve Bayes:

| |
|---|
| **1. The feature set is shuffled and divided into 4 folds.** |
| **a. For each fold:** |
| **i. Training is performed using the training data set. In training the mean and variance of each feature set are calculated.** |
| **ii. Testing is performed for each sample given in input by using the above mentioned formula. Posterior probability is calculated for both classes w.r.t to the input sample.** |

| | |
|---|---|
| iii. | **If the posterior probability of $C_0$ is greater than the posterior probability of $C_1$ the test sample is assigned to $C_0$ and vice versa.** |
| iv. | **Accuracy value is calculated.** |
| **b.** | **Mean Accuracy value is calculated by using the formula mention in equation 4.8.** |

Naïve Bayes classifier has proven efficient results in medical diagnosis and system performance management [59].

The results achieved by implementing the designed system in matlab are discussed in the next chapter along with the comparison.

## 4.6 Summary

This chapter describes and explains the proposed model used to detect the presence of wet aged related macular degeneration. Starts with the preprocessing model where the major concern was to describe the techniques that used to perform noise removal and ROI. Following preprocessing is the segmentation block that consists of two major sub blocks which are k mean color clustering block and morphological operations block. This segmentation block is used to detect the pathological abnormalities that indicate the presence of wet aged related macular degeneration. After segmentation a set of 8 features is extracted depending upon the characteristics of those pathological abnormalities. These features are then used to perform classification using three classifiers. The results obtained from those classifiers is discussed in the next chapter.

# CHAPTER 5 EXPERIMENTALRESULTS

The importance of system accuracy is very important in the medical diagnosis system; any sort of error can cause serious damage. So every system is thoroughly tested and evaluated. This chapter consists of the results and evaluation achieved in detecting Wet aged related macular degeneration. The results achieved compared with the previous research work. My research work proves to be better.

## 5.1 Dataset

The database holds significant importance in the field of medical imaging. It mostly acts as a building block in the comparison and evaluation of different designed image processing algorithms. These designed algorithms are compared on the basis of performance measures like accuracy, sensitivity and specificity.

In our research work the most important part was the collection of the required database. The data set for Wet AMD and OCT images was collected from AFIO (Armed Forces Institute of Ophthalmology), Rawalpindi. The data set provided by them was clinically verified by the medical specialist indicating the abnormalities in the images.

A total of 51 images were collected, out of which 21 are the cases of Wet AMD and 31 were of healthy eyes. The resolution of the images is 759x572. The data set required to detect wet age related macular degeneration is not publicly available.

The dataset is divided into 4 folds, each fold is further divided into training and testing set. The system evaluation is performed using statistical evaluation.Some of the images from the dataset are shown along with the experimental results achieved in the next section.

## 5.2 Experimental Results

The assessment of the proposed medical system is done very carefully. Figure 5.1 shows some of the images from the dataset along with the result achieved after the preprocessing. Column (a) contains original images and column (b) shows the images after the preprocessing.

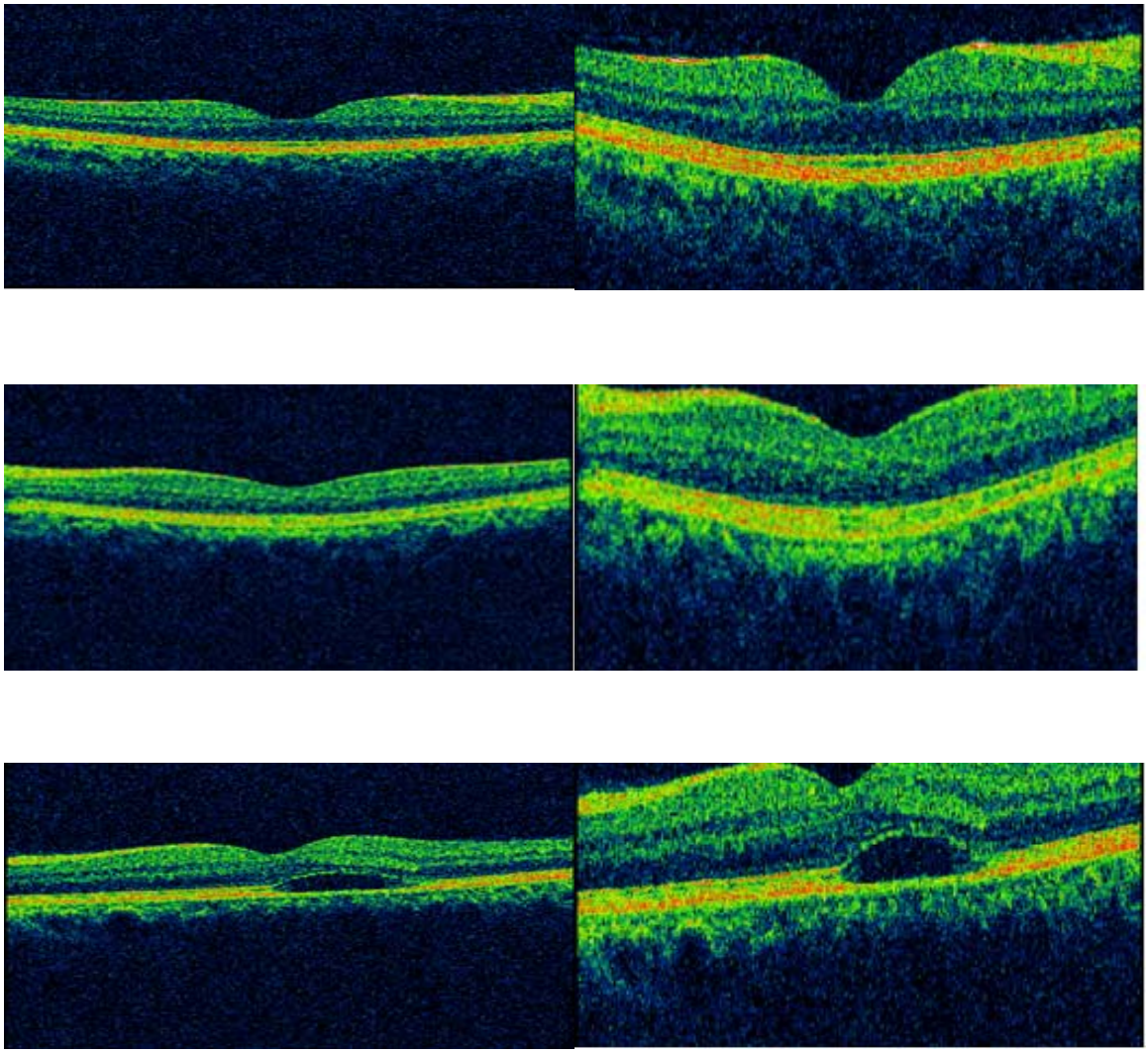

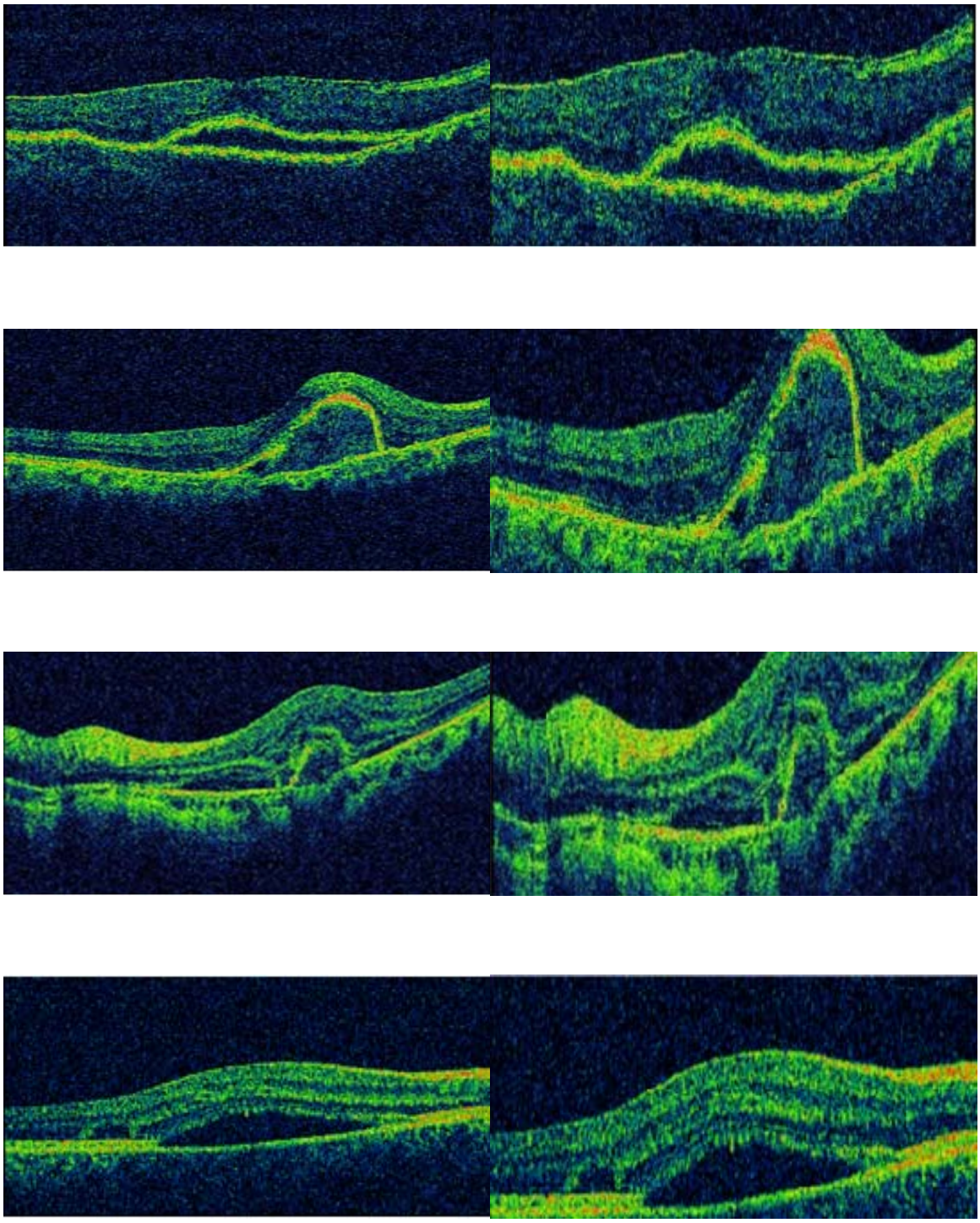

(a) (b)

**Figure 5.1 Column a) Original Images, Column b) Preprocessed Images**

Figure 5.2 shows the result of derived after performing segmentation which consists of k means clustering and morphological operations.Column (a) of figure 5.2 shows images obtained after clustering and column (b) shows the resultant images obtained after performing morphological operations to detect the abnormalities.

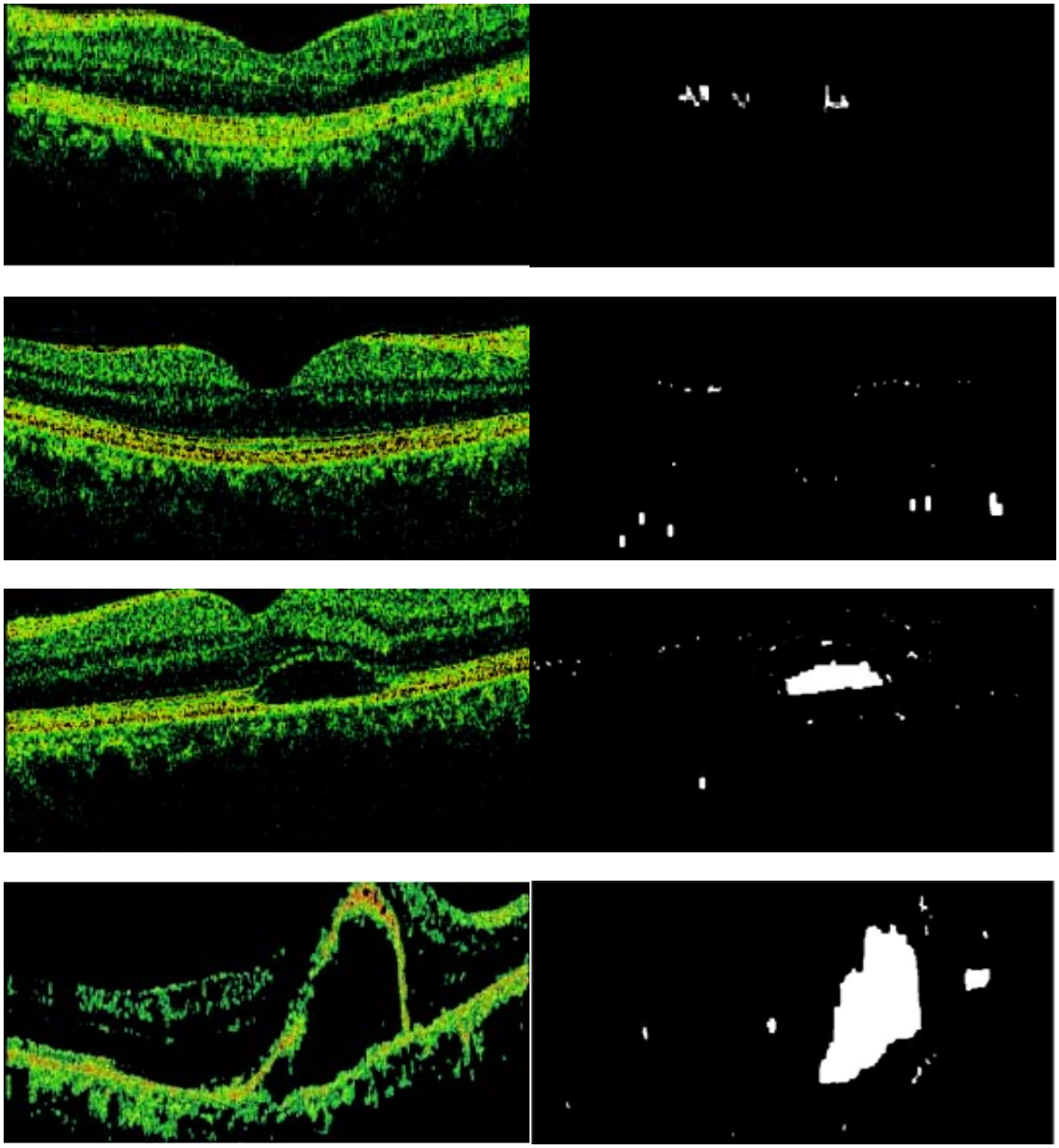

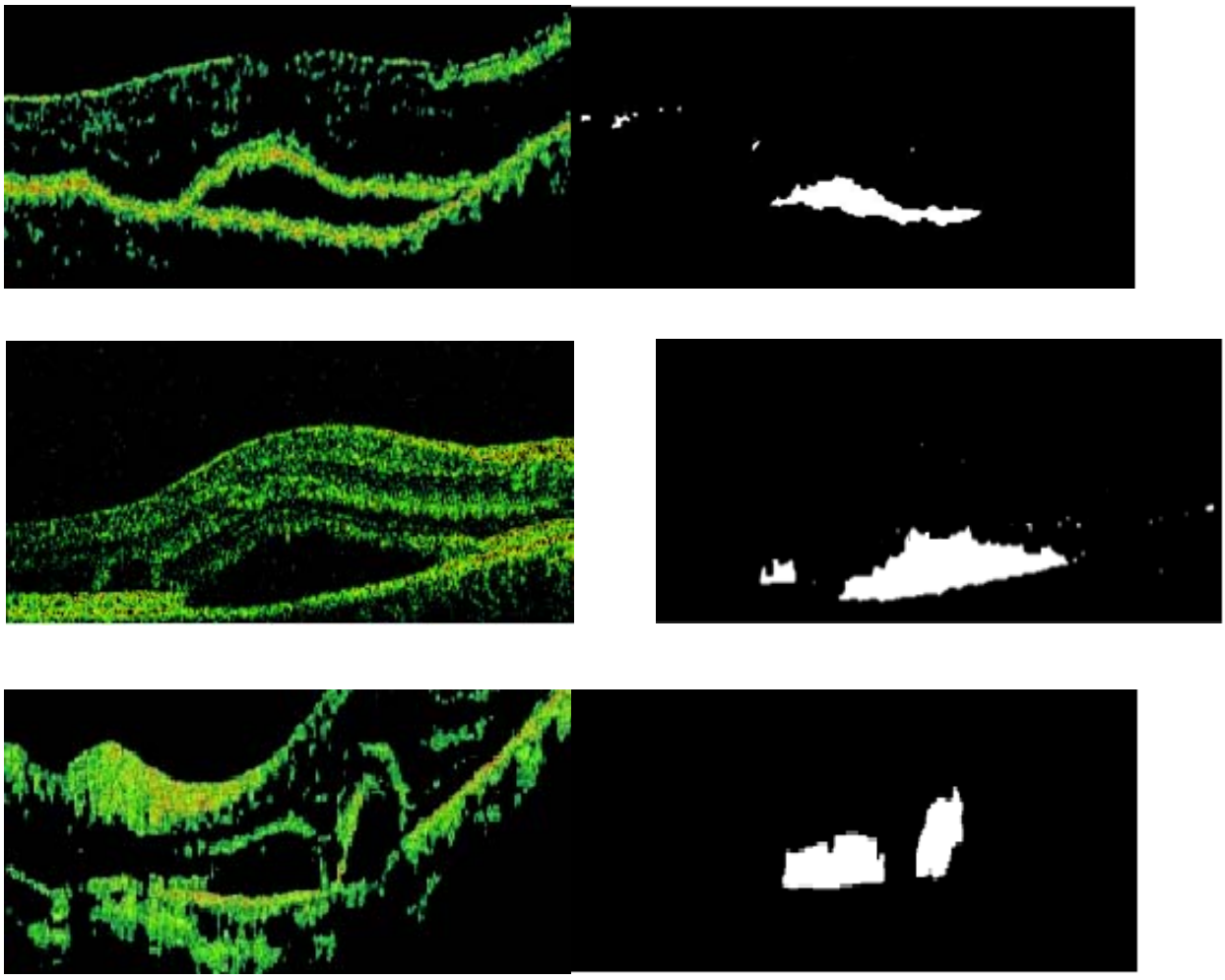

(a) (b)

**Figure 5.2 Column a) Colour Segmentation using k-mean clustering, Column b) PED and CNV detection using Morphological Operations.**

The system evaluation is performed using statistical evaluation measures like accuracy, sensitivity, specificity etc. The performance of the designed system is evaluated using accuracy obtained from each classifier. Aside from accuracy measures sensitivity and specificity are also calculated. All these measures are calculated using Eq. 11, 12, and 13 respectively.

$$Acurracy = \frac{(T_p+T_n)}{(T_p+T_n+F_p+F_n)} \qquad (5.1)$$

$$Sentivity = \frac{(T_p)}{(T_p + F_n)} \quad (5.2)$$

$$Sentivity = \frac{(T_n)}{(T_n + F_p)} \quad (5.3)$$

Where

- $T_p$ stands for true positives, meaning the OCT images correctly classified as wet age related macular degeneration.
- $T_n$stands for true negatives, meaning the OCT images correctly classified as healthy eyes.
- $F_p$ stands for false positives, meaning the OCT images of healthy eyes wrongly classified as wet amd.
- $F_n$ stands for false negatives, meaning the OCT images of wet age related macular degeneration wrongly classified as healthy eyes.

The dataset was divided into 4 folds and the accuracy of each fold is calculated for all three classifiers used in the system.

Statistical measures are performed for each classifier. The achieved measures for KNN, SVM and Naïve Bayes are shown in tables below along with the graphs.

Table 5.1 Statistical Performance measure achieved using proposed system with KNN-Classifier.

| **Number of Folds** | **1** | **2** | **3** | **4** |
|---|---|---|---|---|
| **Accuracy (%)** | 97.37 | 94.74 | 92.63 | 92.31 |
| **Sensitivity (%)** | 100 | 100 | 100 | 100 |
| **Specificity (%)** | 96.3 | 92 | 87.72 | 87.5 |

Table 5.2 Average Values Achieved using proposed system with KNN-Classifier.

| Average Values | |
|---|---|
| **Accuracy (%)** | 94.2 |
| **Sensitivity (%)** | 100 |
| **Specificity (%)** | 91.12 |

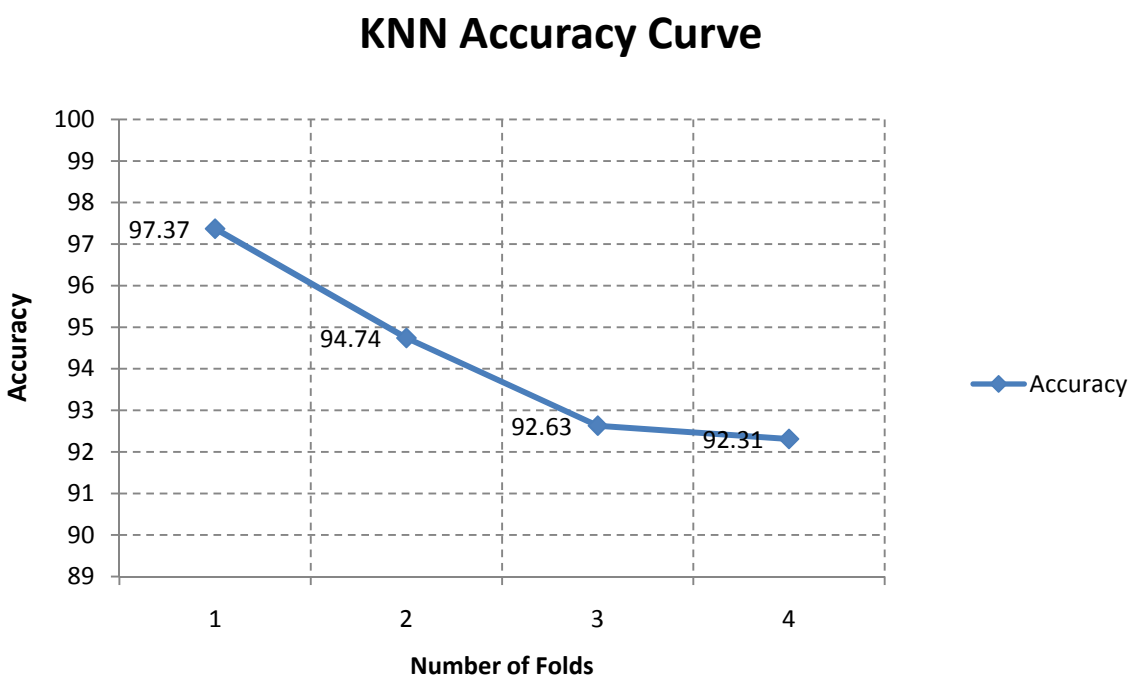


**Figure 5.3 Accuracy curve of KNN Classifier**

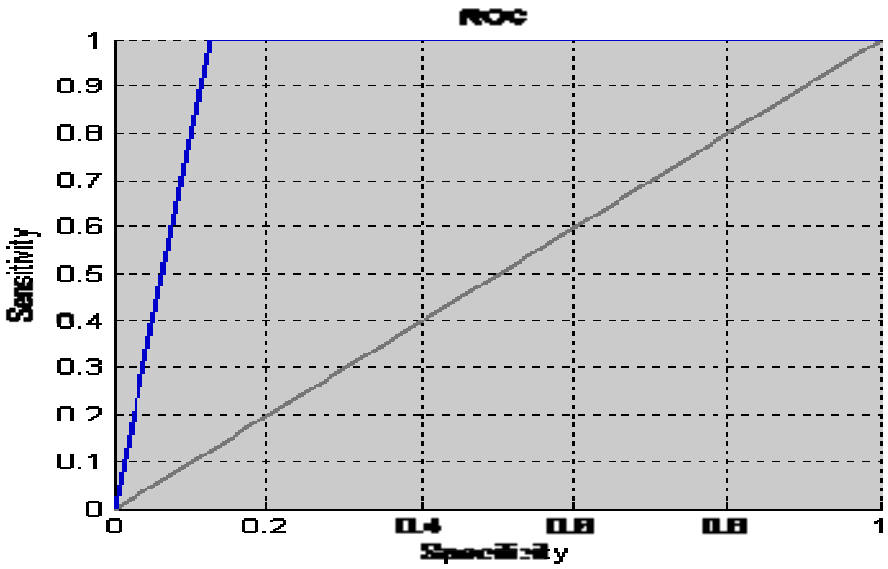


**Figure 5.4 ROC curve of KNN Classifier**

Table 5.3 Confusion Matrix Achieved using proposed system with KNN Classifier

| **Confusion Matrix** | $T_p$ | $F_n$ |
|---|---|---|
| | 0.354 | 0 |
| | $F_p$ | $T_n$ |
| | 0.0574 | 0.5886 |

KNN statistical measures show that it can achieve an accuracy of 94.2% along with sensitivity and specificity of 100% and 92.12%.

Statistical measures achieve by SVM are given below:

Table 5.4 Statistical Performance measure achieved using proposed system with SVM-Classifier.

| **Number of Folds** | **1** | **2** | **3** | **4** |
|---|---|---|---|---|
| **Accuracy (%)** | 92.31 | 84.62 | 92.31 | 100 |

| | | | | |
|---|---|---|---|---|
| **Sensitivity (%)** | 100 | 83.3 | 75 | 100 |
| **Specificity (%)** | 80 | 85.71 | 100 | 100 |

Table 5.5 Average Values Achieved using proposed system with SVM-Classifier.

| **Average Values** | |
|---|---|
| **Accuracy (%)** | 92.13 |
| **Sensitivity (%)** | 90.48 |
| **Specificity (%)** | 93.33 |

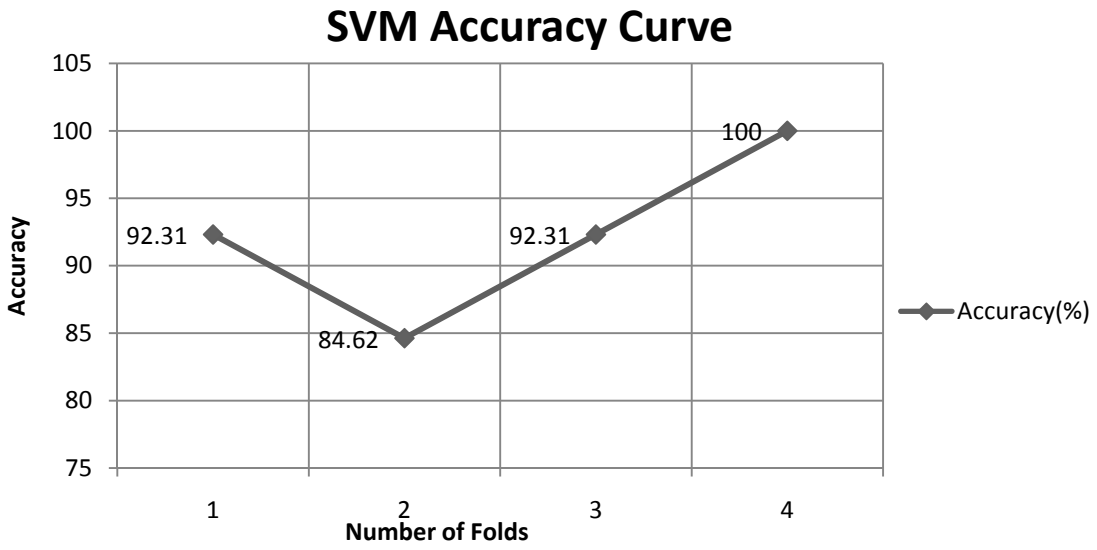


**Figure 5.5 Accuracy curve of SVM Classifier**

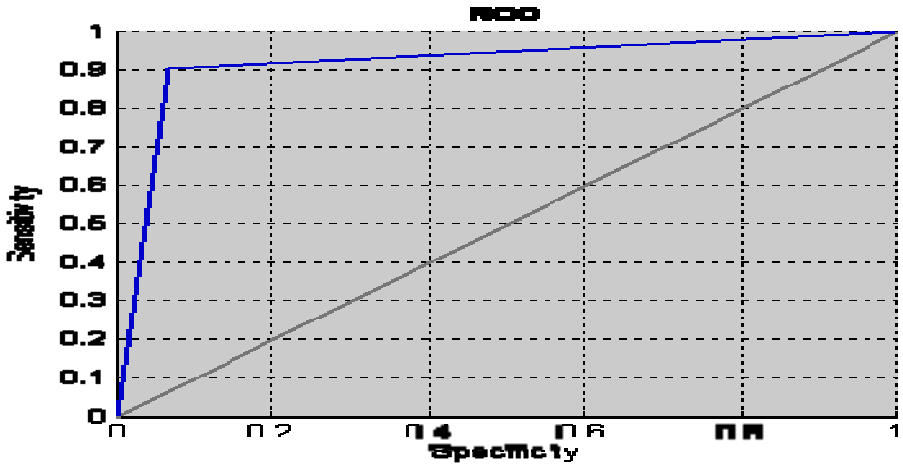


**Figure 5.6 ROC curve of SVM Classifier**

Table 5.6 Confusion Matrix Achieved using proposed system with SVM Classifier

| **Confusion Matrix** | $T_p$ | $F_n$ |
|---|---|---|
| | 0.3725 | 0.0392 |
| | $F_p$ | $T_N$ |
| | 0.0392 | 0.5490 |

Support vector machine can achieve an accuracy of 92.13% along with sensitivity and specificity of 90.48% and 93.33% which is lower then what is achieved using KNN.

Statistical measures achieve by Naïve Bayes Classifier are shown below:

Table 5.7 Statistical Performance measure achieved using proposed system with Naïve Bayes Classifier.

| **Number of Folds** | **1** | **2** | **3** | **4** |
|---|---|---|---|---|
| **Accuracy (%)** | 92.31 | 92.31 | 100 | 100 |
| **Sensitivity (%)** | 100 | 100 | 100 | 100 |

| | | | | |
|---|---|---|---|---|
| **Specificity (%)** | 80 | 87.5 | 100 | 100 |

Table 5.8 Average Values Achieved using proposed system with Naïve Bayes Classifier.

| **Average Values** | |
|---|---|
| **Accuracy (%)** | 96.15 |
| **Sensitivity (%)** | 100 |
| **Specificity (%)** | 93.89 |

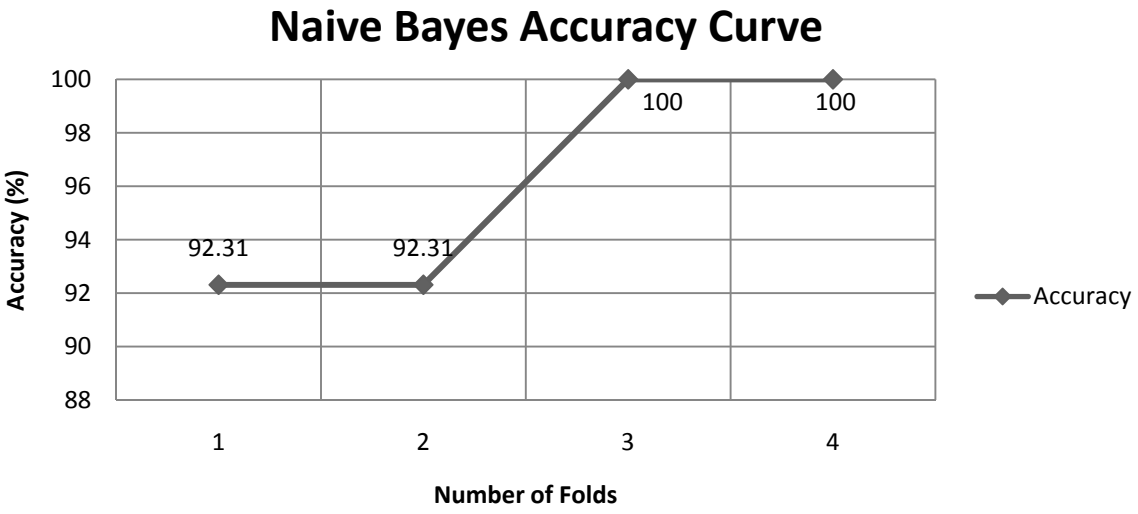


**Figure 5.7 Accuracy curve of Naïve Bayes Classifier**

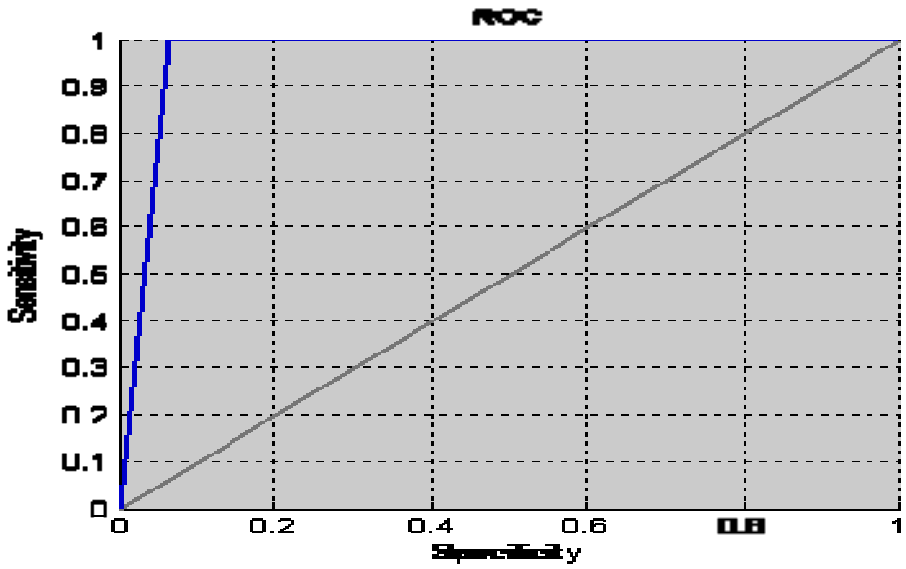


**Figure 5.8 ROC curve of Naïve Bayes Classifier**

Table 5.9 Confusion Matrix Achieved using proposed system with Naïve Bayes Classifier

| **Confusion Matrix** | $T_p$ | $F_n$ |
|---|---|---|
| | 0.3702 | 0 |
| | $F_p$ | $T_n$ |
| | 0.0385 | 0.5913 |

Naïve Bayes classifier can achieve an accuracy of 96.15% along with sensitivity and specificity of 100% and 93.89% which is far better then what is achieved using KNN and SVM. Hence it is considered as the best classifier for the current scenario.

The Comparison of the three classifiers used in our research work on the basis of Accuracy and ROC measures is shown in figures 5.7 and 5.8

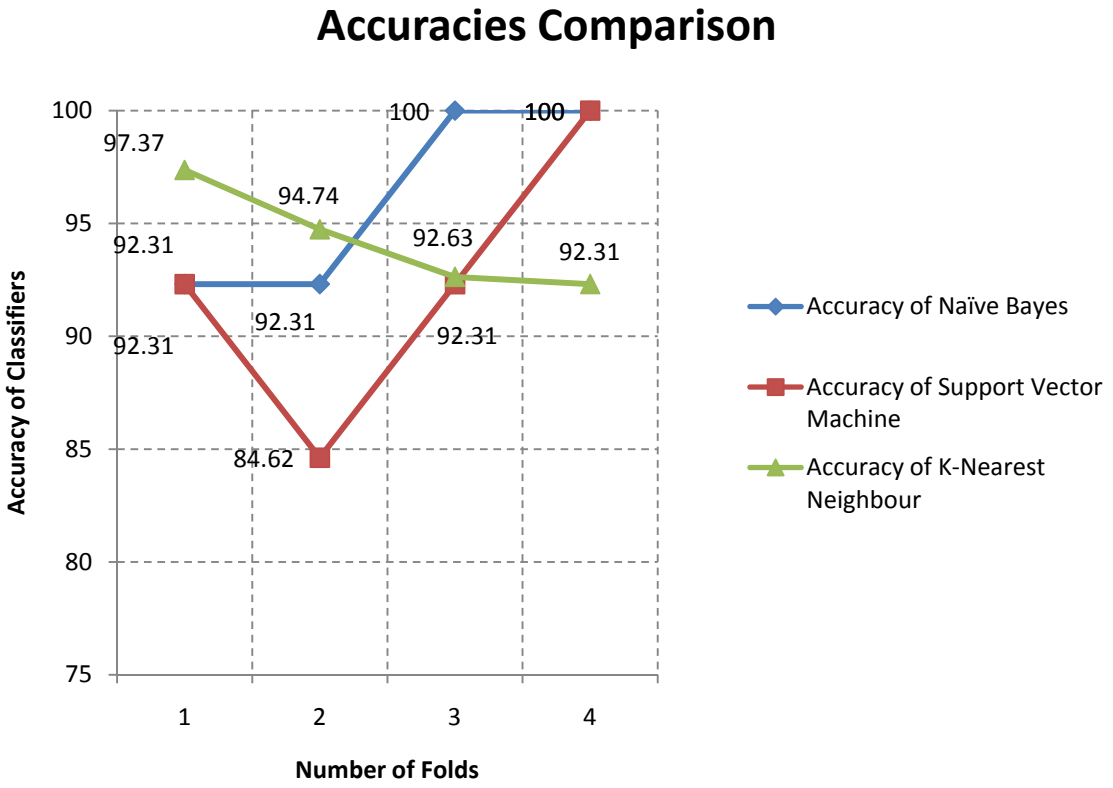


**Figure 5.9 Comparison of Accuracy Achieved from Naïve, KNN, and SVM Classifier**

From the above graph it is quite clear that the accuracy achieved from Naïve Bayes is high as compared to the accuracy obtained by using KNN and SVM Classifier.

The ROC curve achieved using KNN and Naïve Bayes classifier are almost similar so the comparison on ROC curve is done between KNN and SVM.

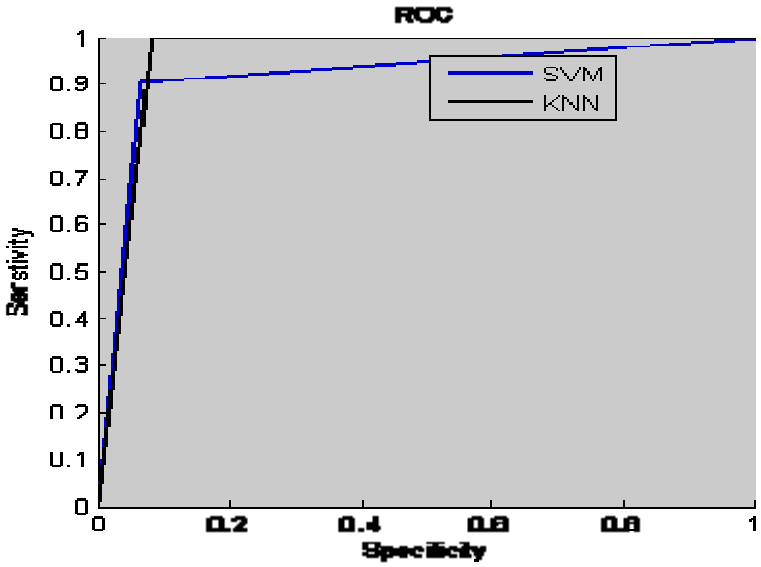


**Figure 5.10 Comparison of ROC Curve Achieved from KNN, and SVM Classifier**

## 5.3 Comparison of Derived Results

The comparison of the designed system with two other approaches used by authors in [48] and [49] is shown in table 5.10. Anam Haq et al [48] obtained the accuracy of 94.23% through SVM classifier while we have achieved an accuracy of 96.15% using Naïve Bayes Classifier. On the other hand Sun Young Lee in [49] had detected only PED using intensity map procedure and has obtained a mean sensitivity and mean specificity of 84%and 81.67%, while our system have detected PEDs and CNVs using morphological operations and achieved the sensitivity and specificity of 100% and 93.75%.

Table 5.10 Comparison of Proposed System with Existing Research Work.

| Author | Method | Detection | Accuracy (%) | Sensitivity (%) | Specificity (%) |
|---|---|---|---|---|---|
| **Sun Young Lee et al. [49]** | Intensity Map | PEDs | _ | 84 | 81.67 |
| **Anam Haq et al. [48]** | Morphological Operations | Wet Aged Related Macular Degeneration (PEDs,CNVs) | 94.23 | 95 | 93.55 |

| | | | | | |
|---|---|---|---|---|---|
| **Proposed Method** | Morphological Operations | Wet Aged Related Macular Degeneration (PEDs,CNVs) | **96.15** | **100** | **93.75** |

## 5.4 Summary

Performance of the designed system was evaluated using different classifiers; the results achieved using the best one was selected for comparison with the current research work. In thesis higher results are achieved using naïve bayes classifier.

# CHAPTER 6 CONCLUSIONS AND FUTURE WORK

## 6.1 Conclusion

Medical image processing is the one of the research fields which is gaining high interest of research engineers and medical doctors as it provides huge help in clinical diagnosis. Our research work focuses on a type of disease which is related to the human eye.

Wet amd is the type of age related macular degeneration. This disease is responsible for a very low percentage of total AMD cases, but nearly 90% of all major vision loss is caused by this type of AMD. In this article, we presented a computerized approach for automatic detection of wet age related macular degeneration. The proposed system performs morphological operations on all OCT images and detects those having pathological abnormalities like CNV and PED. A detailed feature set is created based on the properties of CNV and PED. Extracted features are then passed onto a classifier which classifies between wet age related macular degenerationpatients and healthy patients.

The evaluation of the system is done using database obtained from AFIO using Topcon 100 OCT machine. Our proposed system has achieved greater performance using the naïve Bayes classifier as compared to the one achieved in [47] and [48].

The performance of our system is improved as compared to [48] because of emphasis on selecting sound features and reliable classifiers.

## 6.2 Future Work

The research work can be expanded to the detection of dry age related macular degeneration. Aside from that, the same designed system with different features can be used to detect the following disease:

- Central serous chorioretinopathy

- Macular odema.

This can help in the diagnosis of two very important diseases.Preprocessing of Optical coherence Tomographic images and the segmentation of retinal layers is another area of research on which quality work can be done in short duration and with less effort.

## REFERENCES


[1]. MedicineNet, Image Collection, accessed on December 15, 2013, http://www.medicinenet.com/image-collection/eye_anatomy_detail_picture/picture.htm.

[2]. WebMD, Eye Health Center, accessed on December 15,2013,http://www.webmd.com/eye-health/structures-of-the-eye.

[3]. Rochester Institute of Technology, Center for Imaging Science accessed on December 10, 2013, http://www.cis.rit.edu/people/faculty/montag/vandplite/pages/chap_8/ch8p3.html.

[4]. Kanski J. Clinical Ophthalmology; A Systematic Approach (7th Ed) Butterworth Heinemann (2011)

[5]. Denniston AKO, Murray PI; Oxford Handbook of Ophthalmology (OUP), 2009

[6]. Gerstenblith AT, Rabinowitz MP, Barahimi BI, Fecarotta CM; The Wills Eye Manual: Office and Emergency Room Diagnosis and Treatment of Eye Disease (International Ed), Lippincott, Williams and Wilkins (2012)

[7]. Patient plus Article by Dr. Olivia Scott, accessed on October 10, 2013 http://www.patient.co.uk/doctor/Macular-Disorders.htm.

[8]. Clinical Ophthalmology: A Systematic Approach by Kanski Bowling.

[9]. Patient plus Article accessed on October 15, 2013, http://www.patient.co.uk/doctor/visual-field-defects.

[10]. Check your vision by using amsler grid, accessed on November 20th 2013, http://www.cnib.ca/en/your-eyes/eye-conditions/amd/diagnosing/amsler-grid.

[11]. Patient plus Article by Dr. Olivia Scott, accessed on October 10, 2013 http://www.patient.co.uk/doctor/age-related-macular-degeneration-pro

[12]. National Eye Institute, Facts about Age Related Macular Degeneration, accessed on December 20, 2013, http://www.nei.nih.gov/health/maculardegen/armd_facts.asp

[13]. Adar SD, Klein R, Klein BE, Szpiro AA, Cotch MF, Wong TY, et al. 2010. Air Pollution and the microvasculature: a crosssectional assessment of in vivo retinal images in the population based multiethnic study of atherosclerosis (MESA). PLoS Med 7: e1000372.

[14]. Louwies, T, Int Panis L, Kicinski, M, De Boever P, Nawrot, Tim S, "Retinal Microvascular Responses to Short-Term Changes in Particulate Air Pollution in Healthy Adults". Environmental Health Perspectives (2013).

[15]. Saine PJ. "Fundus Photography: What is a Fundus Camera?" Ophthalmic Photographers' Society. Accessed September 30, 2006.

[16]. Dörr, Jan; Wernecke, KD; Bock, M; Gaede, G; Wuerfel, JT; Pfueller, CF; Bellmann-Strobl, J; Freing, A; Brandt, AU; Friedemann, P (Apr 8, 2011)."Association of retinal and macular damage with brain atrophy in multiple sclerosis.". PLoS ONE 6 (4): e18132. Bibcode:2011PLoSO...618132D.doi:10.1371/journal.pone.0018132. PMID 21494659. Retrieved 21 November 2012.

[17]. Keane, PA; Patel, PJ; Liakopoulos, S; Heussen, FM; Sadda, SR; Tufail, A (September 2012). "Evaluation of age-related macular degeneration with optical coherence tomography.". Survey of ophthalmology 57 (5): 389–414.

[18]. Damestani, Yasaman (2013). "Transparent nanocrystalline yttria-stabilized-zirconia calvarium prosthesis". Nanomedicine (Elsevier Inc.).doi:10.1016/j.nano.2013.08.002. Retrieved September 11, 2013. • Explained by Mohan, Geoffrey (September 4, 2013). "A window to the brain? It's here, says UC Riverside team". Los Angeles Times.

[19]. WJ Walecki et al., Determining thickness of slabs of materials, US Patent 7,116,429, 2006

[20]. Wojtek J. Walecki and Fanny Szondy,"Integrated quantum efficiency, reflectance, topography and stress metrology for solar cell manufacturing", , Sunrise Optical LLC, Proc. SPIE 7064, 70640A (2008).

[21]. Wojciech J. Walecki, Kevin Lai, Alexander Pravdivtsev, Vitali Souchkov, Phuc Van, Talal Azfar, Tim Wong, S. H. Lau and Ann Koo, "Low-coherence interferometric absolute distance gauge for study of MEMS structures", Proc. SPIE 5716, 182 (2005).

[22]. Walecki, W. J., Lai, K., Souchkov, V., Van, P., Lau, S. and Koo, A. (2005),Novel noncontact thickness metrology for backend manufacturing of wide bandgap light emitting devices. physica status solidi (c), 2: 984–989.

[23]. Wojciech Walecki, Frank Wei, Phuc Van, Kevin Lai, Tim Lee, S. H. Lau and Ann Koo, "Novel low coherence metrology for nondestructive characterization of high-aspect-ratio microfabricated and micromachined structures", Proc. SPIE 5343, 55 (2004).

[24]. Guss, G.; Bass, I.; Hackel, R.; Demos, S.G. (November 6, 2007). "High-resolution 3-D imaging of surface damage sites in fused silica with Optical Coherence Tomography". Lawrence Livermore National LaboratoryUCRL-PROC-236270. Retrieved December 14, 2010.

[25]. W Walecki, F Wei, P Van, K Lai, T Lee, Interferometric Metrology for Thin and Ultra-Thin Compound Semiconductor Structures Mounted on Insulating Carriers, CS Mantech Conference, 2004

[26]. Wojciech J. Walecki, Alexander Pravdivtsev, Manuel Santos II and Ann Koo, "High-speed high-accuracy fiber optic low-coherence interferometry for in situ grinding and etching process monitoring", Proc. SPIE 6293, 62930D (2006).

[27]. ZebraOptical Optoprofiler Probe.

[28]. Wojtek J. Walecki and Fanny Szondy, "Fiber optics low-coherence IR interferometry for defense sensors manufacturing", SOLLC, Proc. SPIE 7322, 73220K (2009).

[29]. Dufour, Marc; Lamouche, G.; Gauthier, B.; Padioleau, C.; Monchalin, J.P. (2006). "Inspection of hard-to-reach industrial parts using small diameter probes". SPIE - The International Society for Optical Engineering. Retrieved December 15, 2010.

[30]. Dufour, M. L.; Lamouche, G.; Detalle, V.; Gauthier, B.; Sammut, P. (April 2005). "Low-Coherence Interferometry, an Advanced Technique for Optical Metrology in Industry". Insight - Non-Destructive Testing and Condition Monitoring 47 (4): 216–219.

[31]. Yuanjie Zheng; Vanderbeek, B.; Daniel, E.; Stambolian, D.; Maguire, M.; Brainard, D.; Gee, J., "An automated drusen detection system for classifying age-related macular degeneration with color fundus photographs,"Biomedical Imaging (ISBI), 2013 IEEE 10th International Symposium on , vol., no., pp.144

[32]. A. Rashid, CAREN BELLMANN, VALERIE LE TIEN3, JEAN-CLAUDE KLEIN AND ESTELLE PARRA-DENIS, “Automatic macula detection in human eye fundus

autofluorescence images:Application to eye disease localization",Proceedings of the 10th European Congress of Stereology and Image Analysis, Milan, Italy, June 22-26, 2009

[33]. Agurto, Carla & Barriga, E Simon & Murray, Victor & Nemeth, Sheila & Crammer, Robert & Bauman, Wendall & Zamora, Gilberto & Pattichis, Marios S & Soliz, Peter. "Automatic detection of diabetic retinopathy and age-related macular degeneration in digital fundus images", Investigative ophthalmology & visual science. 2011.

[34]. Alauddin Bhuiyan, C. Karmakar, Di. Xiao, Kotagiri Ramamohanarao, Yogi Kanagasingam,"Drusen quantification for early identification of age related macular degeneration (AMD) using color fundus imaging," Annual International Conference of the IEEE Engineering in Medicine and Biology Society, IEEE Engineering in Medicine and Biology Society, Conference. 2013.

[35]. D.Jayanthi, N.Devi, S.SwarnaParvathi, "Automatic diagnosis of retinal diseases from color retinal images", International Journal of Computer Science and Information Security, Vol. 7, No. 1, 2010

[36]. Prakash Duraisamy, Xiaohui Yuan, El Saba, A. and Sumithra Palanisamy," Contrast enhancement and assessment of OCT images", Proceedings of International Conference on Informatics, Electronics & Vision (ICIEV), 2012 Date: 18-19 May 2012 pp.91-95

[37]. Tao Liu; Zongqing Lu; Qingmin Liao, "Speckle Reduction for Ophthalmic OCT Images Based on Wavelet Filtering Technique," Information Engineering and Computer Science, 2009. ICIECS 2009. International Conference on, vol., no., pp.1,4, 19-20 Dec. 2009.

[38]. Gupta, V.; Chi Chiu Chan; Chueh-Loo Poh; Tzu Hao Chow; Tay Chia Meng; Ng Beng Koon, "Computerized automation of wavelet based denoising method to reduce speckle noise in OCT images," Information Technology and Applications in Biomedicine, 2008. ITAB 2008. International Conference on , vol., no., pp.120,123, 30-31 May 2008.

[39]. G. Franceschetti, V. Pascazio, and G. Schirinzi, ''Iterative homomorphic technique for speckle reduction in syntheticaperture radar imaging,'' J. Opt. Soc. Am. A 12, 686–694 (1995).

[40]. J.M.Schmitt, “Optical coherence tomography(OCT): A Review”, IEEE Journal of Selected Topics in Quantum Electronics, vol. 5, pp. 1205–1215, 1999.Coherence Tomography,” Ophthalmology 116, 488–496 (2009).

[41]. Tapio Fabritius, Shuichi Makita, Masahiro Miura, Risto Myllylä, and Yoshiaki Yasuno (2009) Automated segmentation of the macula by optical coherence tomography. - Optics Express 17 (18), 15659-15669

[42]. D. Cabrera Fernández, H. Salinas, and C. Puliafito, "Automated detection of retinal layer structures on optical coherence tomography images," Opt. Express 13, 10200-10216 (2005).

[43]. S. Chiu, X. Li, P. Nicholas, C. Toth, J. Izatt, and S. Farsiu, "Automatic segmentation of seven retinal layers in SDOCT images congruent with expert manual segmentation," Opt. Express 18, 19413-19428 (2010).

[44]. Qing Dai; Yan Sun, "Automated layer segmentation of optical coherence tomography images," Biomedical Engineering and Informatics (BMEI), 2011 4th International Conference on, vol.1, no., pp.142,146, 15-17 Oct. 2011.

[45]. A. Mishra, A. Wong, K. Bizheva, and D. A. Clausi, “Intra-retinal layer segmentation in optical coherence tomography images,” Opt. Express 17(26), 23719–23728 (2009).

[46]. Dufour PA, Abdillahi H, Ceklic L, Wolf-Schnurrbusch U, Kowal J, “Pathology hinting as the combination of automatic segmentation with a statistical shape model”, MED Image Comput Comput Assist Interv. 2012; 15(Pt.3):599-606.

[47]. Sun Young Lee, Paul F. Stetson, Humberto Ruiz-Garcia, Florian M. Heussen, and SriniVas R. Sadda, “Automated Characterization of Pigment Epithelial Detachment by Optical Coherence Tomography,” IOVS January 2012 53:164-170; published ahead of print December 8, 2011.

[48]. Anam Haq, Fouwad Jamil Mir, Ubaid Ullah Yasin and Shoab. A. Khan, “Classification of Wet Aged Related Macular Degeneration using Optical Coherence Tomographic Images,” Proc. SPIE 9067, Sixth International Conference on Machine Vision (ICMV 2013).

[49]. Dufour, P.A.; De Zanet, S.; Wolf-Schnurrbusch, U.; Kowal, J., "Classification of drusen positions in optical coherence tomography data from patients with age-related macular

degeneration," Pattern Recognition (ICPR), 2012 21st International Conference on, vol., no., pp.2067, 2070, 11-15 Nov. 2012.

[50]. Anil z chitade, Dr. S. k. Katiyar, "Colour based image segmentation using k-means clustering" International Journal of Engineering Science and Technology Vol. 2(10), 2010, 5319-5325.

[51]. Fang Zhao, Yulei Ma, "Medical images processing based on mathematical morphology", ICCASM, July 2012.

[52]. Rafael C. Gonzalez, Richard E.Woods, "Digital image processing, 3rd Edition."

[53]. Bremner D, Demaine E, Erickson J, Iacono J, Langerman S, Morin P, Toussaint G, Output sensitive algorithms for computing nearest neighbor decision boundaries, Discrete and Computational Geometry, 2005, pp. 593–604.

[54]. Cover, T., Hart, P, Nearest-neighbor pattern classification, Information Theory, IEEE Transactions on, Jan. 1967, pp. 21-27.

[55]. Jinho Kim, Byung-Soo Kim, and Silvio Savarese, "Comparing image classification methods: K-nearest-neighbor and support-vector-machines", In Proceedings of the 6th WSEAS international conference on Computer Engineering and Applications, and Proceedings of the 2012 American conference on Applied Mathematics (AMERICAN-MATH'12/CEA'12),2010,pp.133-138.

[56]. Ramteke, R. J,Khachane, Monali , "Automatic Medical Image Classification and Abnormality Detection Using K-Nearest Neighbour," International Journal of Advanced Computer Research;Dec2012, Vol. 2 Issue 6, p190.

[57]. Christoper J.C. Burgers, "A Tutorial on Support Vector Machines for Pattern Recognition", Data Mining and Knowledge Discovery, 1998, pp. 121–167.

[58]. Rish, Irina. "An empirical study of the naive Bayes classifier," IJCAI 2001 Workshop on Empirical Methods in Artificial Intelligence, 2001.

[59]. J. Hellerstein, Jayram Thathachar, and I. Rish, "Recognizing end-user transactions in performance management," In Proceedings of AAAI-2000, Austin, Texas, 2000, pages 596–602,

[60]. Tom M. Mitchell. Machine Learning. McGraw-Hill, 1997.

# APPENDIX

1. **Anam Haq**, Fouwad Jamil Mir, Ubaid Ullah Yasin and Shoab. A. Khan, *"Classification of Wet Aged Related Macular Degeneration using Optical Coherence Tomographic Images,"* Proc. SPIE 9067, Sixth International Conference on Machine Vision (ICMV 2013).